



## RESEARCH ARTICLE

10.1029/2023JG007837

### Special Collection:

The Arctic: An AGU Joint Special Collection

### Key Points:

- Porewater  $\delta^{13}\text{C}-\text{CH}_4$  values of northern bogs and fens differ from each other and correlate with emitted  $\delta^{13}\text{C}-\text{CH}_4$  values
- In addition to peatland type, vascular plant cover, pH, and  $\text{CH}_4$  concentration help explain variation in porewater  $\delta^{13}\text{C}-\text{CH}_4$  values
- The  $\delta^{13}\text{C}-\text{CH}_4$  value for northern peatlands is more sensitive to landscape drying than wetting under permafrost thaw scenarios

### Supporting Information:

Supporting Information may be found in the online version of this article.

### Correspondence to:

M. A. Kuhn,  
kuhn.mckenzie@gmail.com

### Citation:

Kuhn, M. A., Varner, R. K., McCalley, C. K., Perryman, C. R., Aurela, M., Burke, S. A., et al. (2024). Controls on stable methane isotope values in northern peatlands and potential shifts in values under permafrost thaw scenarios. *Journal of Geophysical Research: Biogeosciences*, 129, e2023JG007837. <https://doi.org/10.1029/2023JG007837>

Received 6 OCT 2023  
Accepted 22 JUN 2024

### Author Contributions:




















**Conceptualization:** McKenzie A. Kuhn, Ruth K. Varner, Carmody K. McCalley, Jia Deng, Louis J. Lamit, Virginia I. Rich, Joanne H. Shorter

**Data curation:** McKenzie A. Kuhn, Ruth K. Varner, Carmody K. McCalley, Clarice R. Perryman, Mika Aurela, Sophia A. Burke, Jeffrey P. Chanton, Patrick M. Crill, Jessica DelGreco, Liam Heffernan, Suzanne B. Hodgkins,

© 2024. The Author(s).

This is an open access article under the terms of the [Creative Commons Attribution License](#), which permits use, distribution and reproduction in any medium, provided the original work is properly cited.

# Controls on Stable Methane Isotope Values in Northern Peatlands and Potential Shifts in Values Under Permafrost Thaw Scenarios

McKenzie A. Kuhn<sup>1,2</sup> , Ruth K. Varner<sup>1,2</sup> , Carmody K. McCalley<sup>3</sup> , Clarice R. Perryman<sup>1,2,4</sup>, Mika Aurela<sup>5</sup> , Sophia A. Burke<sup>1,2</sup> , Jeffrey P. Chanton<sup>6</sup> , Patrick M. Crill<sup>7,8</sup>, Jessica DelGreco<sup>2</sup>, Jia Deng<sup>2</sup> , Liam Heffernan<sup>9</sup> , Christina Herrick<sup>2</sup> , Suzanne B. Hodgkins<sup>10</sup> , Cheristy P. Jones<sup>1,2</sup>, Sari Juutinen<sup>5</sup> , Evan S. Kane<sup>11,12</sup> , Louis J. Lamit<sup>13</sup>, Tuula Larmola<sup>14</sup> , Erik Lilleskov<sup>12</sup> , David Olefeldt<sup>15</sup>, Michael W. Palace<sup>1,2</sup>, Virginia I. Rich<sup>11</sup> , Christopher Schulze<sup>15,16</sup> , Joanne H. Shorter<sup>17</sup> , Franklin B. Sullivan<sup>2</sup> , Oliver Sonntag<sup>16</sup>, Merritt R. Turetsky<sup>18</sup>, and Mark P. Waldrop<sup>19</sup> 

<sup>1</sup>Department of Earth Sciences, University of New Hampshire, Durham, NH, USA, <sup>2</sup>Earth Systems Research Center, Institute for the Study of Earth, Oceans and Space, University of New Hampshire, Durham, NH, USA, <sup>3</sup>Gosnell School of Life Science, Rochester Institute of Technology, Rochester, NY, USA, <sup>4</sup>Department of Earth Systems Science, Stanford University, Stanford, CA, USA, <sup>5</sup>Finnish Meteorological Institute, Climate System Research, Helsinki, Finland, <sup>6</sup>Department of Earth Ocean and Atmospheric Science, Florida State University, Tallahassee, FL, USA, <sup>7</sup>Department of Geological Sciences, Stockholm University, Stockholm, Sweden, <sup>8</sup>Bolin Center for Climate Research, Stockholm University, Stockholm, Sweden, <sup>9</sup>Department of Ecology and Genetics/Limnology, Evolutionary Biology Centre, Uppsala University, Uppsala, Sweden, <sup>10</sup>Department of Microbiology, The Ohio State University, Columbus, OH, USA, <sup>11</sup>College of Forest Resources and Environmental Science, Houghton, MI, USA, <sup>12</sup>USDA Forest Service, Northern Research Station, Houghton, MI, USA, <sup>13</sup>Department of Biology, Syracuse University, Syracuse, NY, USA, <sup>14</sup>Natural Resources Institute Finland, Helsinki, Finland, <sup>15</sup>Department of Renewable Resources, University of Alberta, Edmonton, AB, Canada, <sup>16</sup>Département de Géographie, Université de Montréal, Montréal, QC, Canada, <sup>17</sup>Aerodyne Research, Inc., Billerica, MA, USA, <sup>18</sup>Department of Ecology and Evolutionary Biology, University of Colorado Boulder, Boulder, CO, USA, <sup>19</sup>Geology, Minerals, Energy and Geophysics Science Center, U.S. Geological Survey, Menlo Park, CA, USA

**Abstract** Northern peatlands are a globally significant source of methane ( $\text{CH}_4$ ), and emissions are projected to increase due to warming and permafrost loss. Understanding the microbial mechanisms behind patterns in  $\text{CH}_4$  production in peatlands will be key to predicting annual emissions changes, with stable carbon isotopes ( $\delta^{13}\text{C}-\text{CH}_4$ ) being a powerful tool for characterizing these drivers. Given that  $\delta^{13}\text{C}-\text{CH}_4$  is used in top-down atmospheric inversion models to partition sources, our ability to model  $\text{CH}_4$  production pathways and associated  $\delta^{13}\text{C}-\text{CH}_4$  values is critical. We sought to characterize the role of environmental conditions, including hydrologic and vegetation patterns associated with permafrost thaw, on  $\delta^{13}\text{C}-\text{CH}_4$  values from high-latitude peatlands. We measured porewater and emitted  $\text{CH}_4$  stable isotopes, pH, and vegetation composition from five boreal-Arctic peatlands. Porewater  $\delta^{13}\text{C}-\text{CH}_4$  was strongly associated with peatland type, with  $\delta^{13}\text{C}$  enriched values obtained from more minerotrophic fens ( $-61.2 \pm 9.1\%$ ) compared to permafrost-free bogs ( $-74.1 \pm 9.4\%$ ) and raised permafrost bogs ( $-81.6 \pm 11.5\%$ ). Variation in porewater  $\delta^{13}\text{C}-\text{CH}_4$  was best explained by sedge cover,  $\text{CH}_4$  concentration, and the interactive effect of peatland type and pH ( $r^2 = 0.50$ ,  $p < 0.001$ ). Emitted  $\delta^{13}\text{C}-\text{CH}_4$  varied greatly but was positively correlated with porewater  $\delta^{13}\text{C}-\text{CH}_4$ . We calculated a mixed atmospheric  $\delta^{13}\text{C}-\text{CH}_4$  value for northern peatlands of  $-65.3 \pm 7\%$  and show that this value is more sensitive to landscape drying than wetting under permafrost thaw scenarios. Our results suggest northern peatland  $\delta^{13}\text{C}-\text{CH}_4$  values are likely to shift in the future which has important implications for source partitioning in atmospheric inversion models.

**Plain Language Summary** Peatlands are abundant across the boreal-Arctic landscape and are important sources of methane, a powerful greenhouse gas. The amount of methane emitted into the atmosphere depends on multiple factors including the organic material being decomposed and the microbial processes (“pathways”) that produce methane. The different pathways of methane production leave distinct fingerprints (“stable carbon isotopes”) on methane that provide information on how that methane was formed and help to trace methane in the atmosphere back to its ground source. We looked at how stable carbon isotopes change across five northern peatland locations and wanted to know what controls those changes. We found that stable carbon isotopes differ between bogs and fens and are further

Sari Juutinen, Evan S. Kane,  
 Tuula Larmola, Erik Lilleskov,  
 David Olefeldt, Michael W. Palace,  
 Virginia I. Rich, Christopher Schulze,  
 Joanne H. Shorter, Franklin B. Sullivan,  
 Oliver Sonnentag, Merritt R. Turetsky,  
 Mark P. Waldrop

**Formal analysis:** McKenzie A. Kuhn,  
 Ruth K. Varner, Carmody K. McCalley,  
 Clarice R. Perryman, Jeffrey P. Chanton,  
 Christina Herrick, Suzanne B. Hodgkins,  
 Cheristy P. Jones, Louis J. Lamit, Michael  
 W. Palace, Joanne H. Shorter, Franklin  
 B. Sullivan

**Funding acquisition:** Ruth K. Varner,  
 Jeffrey P. Chanton, Louis J. Lamit,  
 Virginia I. Rich

**Investigation:** Ruth K. Varner, Carmody  
 K. McCalley, Clarice R. Perryman, Sophia  
 A. Burke, Jeffrey P. Chanton,  
 Jessica DelGreco, Christina Herrick,  
 Suzanne B. Hodgkins, Louis J. Lamit,  
 Michael W. Palace, Virginia I. Rich,  
 Franklin B. Sullivan

**Methodology:** McKenzie A. Kuhn, Ruth  
 K. Varner, Carmody K. McCalley, Clarice  
 R. Perryman, Mika Aurela, Sophia  
 A. Burke, Jeffrey P. Chanton, Patrick  
 M. Crill, Jia Deng, Liam Heffernan,  
 Christina Herrick, Suzanne B. Hodgkins,  
 Sari Juutinen, Evan S. Kane, Louis  
 J. Lamit, Tuula Larmola, Erik Lilleskov,  
 David Olefeldt, Michael W. Palace,  
 Virginia I. Rich, Christopher Schulze,  
 Joanne H. Shorter, Franklin B. Sullivan,  
 Oliver Sonnentag, Merritt R. Turetsky,  
 Mark P. Waldrop

**Project administration:** Ruth K. Varner,  
 Suzanne B. Hodgkins, Virginia I. Rich

**Resources:** Ruth K. Varner, Mika Aurela,  
 Jeffrey P. Chanton, Patrick M. Crill,  
 Liam Heffernan, Sari Juutinen, Evan  
 S. Kane, Louis J. Lamit, Tuula Larmola,  
 Erik Lilleskov, David Olefeldt, Virginia  
 I. Rich, Christopher Schulze, Joanne  
 H. Shorter, Oliver Sonnentag, Merritt  
 R. Turetsky, Mark P. Waldrop

**Software:** Suzanne B. Hodgkins

**Supervision:** Ruth K. Varner, Virginia  
 I. Rich

**Validation:** Carmody K. McCalley,  
 Clarice R. Perryman, Christina Herrick,  
 Suzanne B. Hodgkins

**Visualization:** McKenzie A. Kuhn, Ruth  
 K. Varner, Clarice R. Perryman, Cheristy  
 P. Jones

**Writing – original draft:** McKenzie  
 A. Kuhn

**Writing – review & editing:** McKenzie  
 A. Kuhn, Ruth K. Varner, Carmody  
 K. McCalley, Clarice R. Perryman,  
 Mika Aurela, Sophia A. Burke, Jeffrey  
 P. Chanton, Patrick M. Crill,  
 Jessica DelGreco, Jia Deng,  
 Liam Heffernan, Christina Herrick,  
 Suzanne B. Hodgkins, Cheristy P. Jones,  
 Sari Juutinen, Evan S. Kane, Louis  
 J. Lamit, Tuula Larmola, Erik Lilleskov,  
 David Olefeldt, Michael W. Palace,  
 Virginia I. Rich, Christopher Schulze,  
 Joanne H. Shorter, Franklin B. Sullivan,

controlled by soil pH and the abundance of sedge vegetation present. We used this information to test how stable carbon isotopes from northern peatlands might change as the landscape becomes wetter or drier due to the impacts of climate change. We found that peatland stable carbon isotopes are most sensitive to potential landscape drying opposed to wetting which has important implications for improving methane emission models.

## 1. Introduction

Northern peatlands store ~20% of the Earth's soil carbon (Hugelius et al., 2020), and are globally significant yet uncertain sources of methane (CH<sub>4</sub>). The rates and sources of CH<sub>4</sub> emission from northern peatlands are vulnerable to climate warming and permafrost thaw-driven transitions in landscape composition (Turetsky et al., 2020; Varner et al., 2022). Relatively minor changes in CH<sub>4</sub> emissions from peatlands alter the radiative forcing impact (i.e., climbing warming potential) on decadal scales (Frolking et al., 2006), making it critical to better constrain current and future estimates of CH<sub>4</sub> emissions. However, estimates of current annual CH<sub>4</sub> emissions vary among different modeling approaches, which also limits our ability to predict future CH<sub>4</sub> emissions. Bottom-up global and regional models that use field data or process-based models tend to find higher annual emissions (Bansal, Post van der Burg, et al., 2023; Bloom et al., 2017; Peltola et al., 2019; Treat et al., 2018) than top-down inversion models that use atmospheric CH<sub>4</sub> concentrations, chemical transport models, and stable carbon isotopes (δ<sup>13</sup>C-CH<sub>4</sub>) to trace annual CH<sub>4</sub> emissions to ground sources (Basu et al., 2022; Bruhwiler et al., 2021; Oh et al., 2023). Improving our understanding of the underlying mechanisms controlling δ<sup>13</sup>C-CH<sub>4</sub> values could help bridge the gap between modeling approaches and reduce annual emission uncertainties. Top-down models use δ<sup>13</sup>C-CH<sub>4</sub> to separate contributions of atmospheric CH<sub>4</sub> from fossil fuel combustion and biogenic (i.e., microbial) sources, including peatlands (Basu et al., 2022; Oh et al., 2023; Stevens & Engelkemeir, 1988). Some process-based bottom-up models use δ<sup>13</sup>C-CH<sub>4</sub> to partition the underlying mechanisms of CH<sub>4</sub> production and consumption, leading to more accurate simulations of CH<sub>4</sub> emissions (Deng et al., 2017). Only a handful of bottom-up models (empirical and process-based) simulate δ<sup>13</sup>C-CH<sub>4</sub> values which can then be used to improve top-down models (e.g., Ganesan et al., 2018; Oh et al., 2022).

Microbial CH<sub>4</sub> production pathways produce CH<sub>4</sub> with different δ<sup>13</sup>C values that fall within distinctive ranges (Popp et al., 1999; Whiticar et al., 1986). Acetoclastic methanogenesis, the fermentation of acetate into CH<sub>4</sub> and CO<sub>2</sub>, typically produces δ<sup>13</sup>C values between −70 and −30‰ and occurs in environments with labile organic substrates, such as graminoid-dominated, nutrient-rich peatlands and wetlands (e.g., fens, swamps, and marshes) with *Carex* and *Eriophorum* species. Hydrogenotrophic methanogenesis, the reduction of CO<sub>2</sub> with H<sub>2</sub>, produces more depleted δ<sup>13</sup>C values between −100 and −60‰ and is often dominant in environments with less labile organic substrates, few vascular plants, lower water table levels, and lower redox conditions (Conrad, 2020; Hines et al., 2008; Hodgkins et al., 2014). These environments include *Sphagnum*-dominated bogs and elevated permafrost bogs such as palsas and permafrost peat plateaus (Olefeldt et al., 2021a, 2021b). Notably, other production pathways, such as methylotrophic methanogenesis can also make up a portion of emitted CH<sub>4</sub> (Dalcin Martins et al., 2017) with a different range of δ<sup>13</sup>C-CH<sub>4</sub> that falls within the range of hydrogenotrophy (−83‰ to −72‰; Penger et al., 2012), but the relative importance of methylotrophy remains unconstrained (Conrad, 2020). The δ<sup>13</sup>C value of porewater CO<sub>2</sub> can be used alongside δ<sup>13</sup>C-CH<sub>4</sub> to calculate the apparent fractionation factors (α) for methanogenesis, which provides additional insights into microbial production pathways (Chanton et al., 2005). δ<sup>13</sup>C-CH<sub>4</sub> values are also altered by CH<sub>4</sub> consumption (methanotrophy), which enriches isotopic values (Coleman et al., 1981). Plant-mediated diffusion of CH<sub>4</sub> also fractionates isotopes, leading to depleted values in emitted CH<sub>4</sub> compared to porewater (Chanton et al., 2005; Popp et al., 2000). However, the hydrogen isotopic value of CH<sub>4</sub>, deuterium (δD-CH<sub>4</sub>), can be paired with δ<sup>13</sup>C-CH<sub>4</sub> to partition fractionation effects of oxidation and plant transport (Chanton et al., 2005) and more accurately assess patterns in CH<sub>4</sub> cycling. Despite the influence of oxidation and plants on δ<sup>13</sup>C-CH<sub>4</sub> values, patterns in both porewater and emitted δ<sup>13</sup>C-CH<sub>4</sub> values tend to show distinct differences between bog and fen habitats that suggest a shift from predominantly hydrogenotrophic to acetoclastic production (Hines et al., 2008; Hornibrook, 2009; McCalley et al., 2014). However, the reported range of emitted δ<sup>13</sup>C-CH<sub>4</sub> values for northern peatlands remains broad, and partly overlapping between peatland types, making it challenging to scale values across large areas, identify key environmental drivers of source changes, and use in inversion models to partition CH<sub>4</sub> sources.

Oliver Sonnentag, Merritt R. Turetsky,  
Mark P. Waldrop

Historically, the mixed atmospheric  $\delta^{13}\text{C-CH}_4$  value used for microbial wetland sources was simplistically represented by a value of  $\sim -60\text{‰}$  for the entire globe (Bousquet et al., 2006; Houweling et al., 2000; Mikaloff Fletcher et al., 2004; Monteil et al., 2011; Rigby et al., 2012). More recently, models have differentiated wetland/peatland  $\delta^{13}\text{C-CH}_4$  values across latitudes (boreal-Arctic:  $-68 \pm 4\text{‰}$ , Tropics:  $-57 \pm 3\text{‰}$ ; Oh et al., 2022; Ganesan et al., 2018), better representing latitudinal differences in  $\text{C}_3$  and  $\text{C}_4$  plant distribution and related isotopic fraction of plant organic matter (Brownlow et al., 2017). However, the empirical data used to model high-latitude  $\delta^{13}\text{C-CH}_4$  values supporting these studies are based on limited field measurements from northern peatlands and the modeled spatial variation of  $\delta^{13}\text{C-CH}_4$  values is not well constrained (Ganesan et al., 2018; Oh et al., 2022). Furthermore, warming and permafrost thaw can alter landscape hydrology and vegetation (Lawrence et al., 2015; Turetsky et al., 2020; Zhang et al., 2022) and thus change the  $\text{CH}_4$  production and consumption pathways, shifting  $\delta^{13}\text{C-CH}_4$  values. However, these changes are not currently considered in most  $\delta^{13}\text{C-CH}_4$  models, and more field-based measurements are required to improve our understanding of the controls on northern peatland  $\delta^{13}\text{C-CH}_4$  values and related spatial patterns.

We visited five northern peatland complexes across four countries, with sites located within the sporadic and discontinuous permafrost zones (10 to  $<50\%$  and  $50\%$ – $90\%$  landscape permafrost cover, respectively), representing a range of climates and permafrost characteristics. We collected data on vegetation composition, atmospheric  $\text{CH}_4$  and  $\delta^{13}\text{C-CH}_4$  fluxes, porewater pH, and porewater  $\text{CH}_4$  and  $\text{CO}_2$  concentrations and stable isotope composition ( $\delta^{13}\text{C-CH}_4$ ,  $\delta\text{D-CH}_4$ , and  $\delta^{13}\text{C-CO}_2$ ). Our first objective was to model the variation in stable isotopes of porewater and emitted  $\text{CH}_4$  across diverse peatland habitats. We hypothesized that variation in  $\delta^{13}\text{C-CH}_4$  values would be best explained by vascular plant cover and peatland type, broadly defined by permafrost presence, hydrology, and vegetation characteristics (Olefeldt et al., 2021a, 2021b). For our second objective, we then sought to use these model results to assess the sensitivity of northern peatland atmospheric values to vegetation shifts and soil wetting and drying scenarios associated with projected permafrost thaw.

## 2. Study Locations and Methods

### 2.1. Study Locations and Peatland Classification

Peatlands within each of the five study locations were classified according to Olefeldt et al. (2021a, 2021b) and were split into three classes based on permafrost presence, hydrology (i.e., soil saturation and water table), and vegetation type; the combination of which lends to different  $\text{CH}_4$ -emitting potentials (Kuhn et al., 2021). The three peatland types characterized in this study include permafrost-free fens, permafrost-free bogs, and permafrost-affected bogs (i.e., bogs underlain by permafrost in the top 2 m; Olefeldt et al., 2021a, 2021b). These three wetland types represent a gradient of increasing possibility of external hydrological inputs. Permafrost bogs have the smallest inputs of external surface water due to their raised (or perched) nature and receive water mainly from rain (i.e., ombrotrophic). Permafrost-free bogs have slightly more hydrological (near-surface) connections than permafrost bogs but remain mostly ombrotrophic. Fens are minerotrophic (i.e., influenced by groundwater inputs) peatlands with greater water exchange and less acidity than bogs and permafrost bogs. Vegetation in these peatlands depends on nutrient status and hydrologic connectivity, with a dominance of graminoids, forbs, and trees in nutrient-rich fen ecosystems and more dominant ever-green shrubs and mosses in nutrient-poor bog systems (Olefeldt et al., 2021a, 2021b; Rydin et al., 2013) (Figure S1 in Supporting Information S1). Permafrost bogs often have the lowest water tables of the peatland types due to the presence of permafrost in the near-surface which causes the surface to be elevated. Permafrost bogs are dominated by lichens, *Sphagnum* mosses, woody/ericaceous shrubs, and on occasion, trees (Olefeldt et al., 2021a, 2021b).

We visited each of the five northern field sites once in July, between 2015 and 2019 (Figure 1; Table S1 in Supporting Information S1). The peatland complexes span mean average annual temperatures (MAAT; 1970–2000) of  $-5.2$  to  $-0.6^\circ\text{C}$  (Fick & Hijmans, 2017), have mean annual precipitation (MAP) between  $\sim 270$  and  $\sim 390$  mm, and are located across sporadic and discontinuous permafrost zones (Table S1 in Supporting Information S1). Detailed site descriptions are provided in the respective literature for Abisko (Hodgkins et al., 2014; McCalley et al., 2014), the Alaska Peatland Experiment (APEX; Kane et al., 2010), Kaamanen (Heiskanen et al., 2021), Lutose (Heffernan et al., 2022), and Smith Creek (Schulze et al., 2023). Brief descriptions are provided below and in Table S1 of Supporting Information S1:

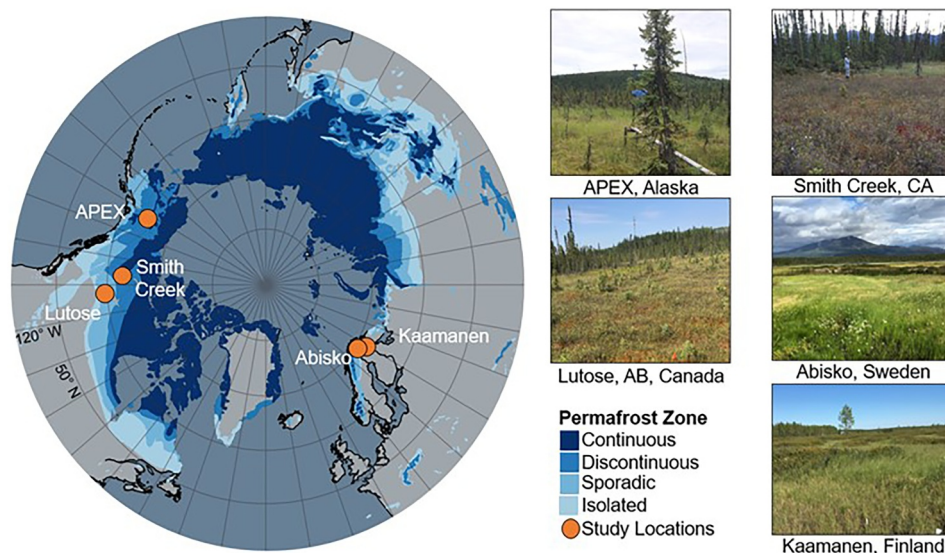


**Figure 1.** The five study locations (orange circles) across the northern region. Permafrost zones, indicated by blue shadings, are from Brown et al. (2002). Representative photos of the five study sites are shown to the right of the map.

**Abisko** (68.35°N, 19.05°E): Stordalen Mire, located near Abisko in northern Sweden, is a thawing permafrost peatland. The peatland complex is composed of elevated, treeless permafrost palsas (i.e., permafrost bogs; dominated by dwarf shrubs, feather mosses, and lichen), *Sphagnum*-dominated bogs, and sedge (predominantly *Eriophorum angustifolium*)-dominated fens. The average peat depth at the site is 1–3 m (Åkerman & Johansson, 2008). The MAAT at the site has steadily been increasing and is often above 0.0°C (average 0.3°C; 1991–2015) and MAP over that same period is ~340 mm (Kuhn et al., 2018).

**APEX** (64.70°N, 148.31°W): The Alaska Peatland Experiment (APEX) is located near the Bonanza Creek Long-Term Ecological Research Forest, near Fairbanks, Alaska, USA. The site is classified as a permafrost-free rich fen, dominated by sedge (*Carex atherodes*), marsh cinquefoil (*Potentilla palustris*), water horsetail (*Equisetum fluviatile*), and brown mosses (*Drepanocladus aduncus* and *Hamatocaulis vernicosus*). Also part of the APEX suite of sites is a black spruce dominated permafrost bog underlain by relatively thin and young (Holocene aged) permafrost, with adjacent thermokarst bogs resulting from surface permafrost thaw over the past several hundred years. Peat depth at the site is ~1–2 m (Euskirchen et al., 2024; Kane et al., 2010). MAAT and MAP at APEX are –2.3°C (1970–2000) and 269 mm (1917–2000), respectively (Hinzman et al., 2006).

**Kaamanen** (69.14°N, 27.27°E): Kaamanen is a patterned mesotrophic patterned fen located in northern Finland, comprising low-lying flarks (wet fen habitats) and elevated strings (bog-like habitats). Fens at the site have high water tables and are dominated by sedge species (*Eriophorum angustifolium*, *Trichophorum cespitosum*, *Carex* spp.) and brown mosses (e.g., *Scorpidium scorpioides*). The bog-like elevated strings are dominated by *Ericaceae* shrubs, feather mosses, and *Sphagnum* mosses, have lower water table depths, and frozen ground is present for most of the growing season (Heiskanen et al., 2021). The peat depth at the site is 1–2 m (Piilo et al., 2020). MAAT and MAP at the site are –0.7°C (1970–2000; –0.4°C for 1981–2010) and 472 mm, respectively (Pirinen, 2012).

**Smith Creek** (63.15°N, 123.26°W): The Smith Creek peatland complex is located near Pehdzeh Ki (also referred to as Wrigley), Northwest Territory, Canada. The site is a permafrost peatland complex with a mix of treed, permafrost peat plateaus (i.e., permafrost bogs) and permafrost-free, saturated fens and bogs. Vegetation on the permafrost bogs is characterized by open canopy, stunted black spruce (*Picea mariana*), Labrador tea (*Rhododendron groenlandicum*), woody shrubs, lichens (*Cladonia* spp.), and patches of dry-adapted *Sphagnum fuscum*. Fens at this site have water tables above the ground surface and are dominated by open water, but also patches of *Carex* spp. and *Potentilla palustris* (marsh cinquefoil). Bogs are dominated by *Sphagnum fuscum* and *Sphagnum divinum/medium* (not differentiated), bog-rosemary (*Andromeda polifolia*), leatherleaf (*Chamaedaphne calyculata*), and hare's tail cottongrass (*Eriophorum vaginatum*). Newly formed “thermokarst wetlands” at the site have higher water tables than bogs and are composed of *Sphagnum riparium* and rannock rush (*Scheuchzeria*

*palustris*). We classified these newly formed thermokarst wetlands as fens under the definitions by Olefeldt et al. (2021a, 2021b). Peat depth at the site is ~1.5 m (Schulze et al., 2023). MAAT and MAP are  $-5.1^{\circ}\text{C}$  and ~360 mm, respectively (1970–2000).

**Lutose** ( $59.49^{\circ}\text{N}$ ,  $117.18^{\circ}\text{W}$ ): The Lutose field site is located in northern Alberta, Canada. The site comprises similar peatland types and vegetation as the Smith Creek Site (~700 km away; see description above). The site is located at the southern extent of permafrost in boreal Western Canada, an area where total permafrost loss from plateaus is projected to occur by 2050 (Chasmer & Hopkinson, 2017). Peat depth at the site is 5–6 m (Heffernan et al., 2020). MAAT and MAP are  $-1.6^{\circ}\text{C}$  and 391 mm, respectively (1970–2000).

## 2.2. Field Sampling of Porewater Chemistry and Emitted Isotopes

Individual plots ( $\sim 1 \times 1$  m) at each site were classified into the BAWLD peatland types described above (Olefeldt et al., 2021a, 2021b). Sampling locations were chosen to cover a range of vegetation and microhabitat covers and were limited by boardwalk location when boardwalks were present. The number of porewater sampling locations (145) was greater than the number of chamber flux sampling locations (15; see Table S2 in Supporting Information S1). For vegetation percent cover, individual species were estimated across 16 sub-squares within the  $1 \times 1$  m quadrat at each plot. Species were then coarsely classified as lichen, *Sphagnum* moss, other moss species, shrub, vascular plants (i.e., graminoids; herein referred to as sedges), tree, or other (mostly forbs). Percent cover of muck (i.e., bare peat) and open water were also recorded. Summaries of the average vegetation cover for each peatland type across the five circumpolar locations are provided in Figure S1 of Supporting Information S1.

Porewater samples were taken from 145 plots every 10 cm at depths between 0 and 60 cm below the peat surface (Figure S2 in Supporting Information S1; Table S2 in Supporting Information S1), for quantification of pH, dissolved concentrations of  $\text{CH}_4$  and  $\text{CO}_2$ , and their respective isotopes ( $\delta^{13}\text{C-CH}_4$ ,  $\delta\text{D-CH}_4$ , and  $\delta^{13}\text{C-CO}_2$ ). Porewater samples were collected using a 3 mm inner diameter perforated stainless steel sipper inserted immediately before sampling. Porewater samples were collected in depth order from the shallowest to deepest sample and between samples 60 mL of porewater was collected and discarded to ensure all sampled water (see below) was from the correct depth. Due to variations in the water table depth across peatland types and individual plots, all six depths were not always sampled as we only sampled below the water table (Figure S2 in Supporting Information S1). For paired porewater samples and flux measurements, porewater samples were taken adjacent to collars to not disturb the area within the collars. Porewater pH was measured on-site with an Oakton Waterproof pHTestr 10 (Eutech Instruments, Woburn, MA). For porewater  $\text{CH}_4$  concentrations, two 30 mL samples of porewater were equilibrated with 30 mL of ambient air in a 60 mL polypropylene syringe by shaking each syringe for ~2 min (Bansal, Creed, et al., 2023). Equilibrated headspace air samples were injected into pre-evacuated 30 mL vials equipped with rubber butyl septa and crimp caps for storage before analysis. A subset of porewater gas samples ( $n = 25$ ) at all sites except for Abisko were sampled for  $\delta\text{D-CH}_4$ . For paired dissolved  $\text{CH}_4$  and  $\text{CO}_2$  samples, 25 mL of porewater from each sampled depth was injected into a pre-evacuated 30-mL vial acidified with 1 mL of 20%  $\text{H}_3\text{PO}_4$ . Limited measurements were taken at Abisko and included pH, vegetation, porewater/emitted  $\delta^{13}\text{C-CH}_4$  and  $\text{CH}_4$  concentrations, but did not include  $\text{CO}_2$  concentrations/isotopes or  $\delta\text{D-CH}_4$ .

Emitted  $\text{CH}_4$  fluxes and associated  $\delta^{13}\text{C-CH}_4$  were measured at a subset of pre-established plots across all locations ( $n = 15$  and 13 for  $\text{CH}_4$  flux measurements and emitted  $\delta^{13}\text{C-CH}_4$  measurements, respectively). Emitted fluxes were measured using a static chamber with headspace sampling with a plastic syringe every 20 min over an hour. Flux measurement set-ups previously existing at each site were adopted at all sites (Heffernan et al., 2022; Heiskanen et al., 2021; Schulze et al., 2023; Turetsky et al., 2008). The different chamber volumes at each site (size range: 48–144 L) were accounted for in flux calculations. At all locations, chambers were gently placed on pre-installed collars while standing on boardwalks to minimize disturbance to the soil. Chambers were sealed to the collars by filling the collar grooves with water after placing the chamber.  $\delta^{13}\text{C-CH}_4$  fluxes were determined by leaving the chamber on for 40–60 min to ensure sufficiently high concentrations for analysis (see below). In Abisko, flux and emitted isotope data were measured with autochambers attached to a quantum cascade laser spectrometer (Aerodyne; full methods described in McCalley et al., 2014). Abisko autochamber data presented here represent the July 2015 monthly averages per peatland type. The  $\delta^{13}\text{C-CH}_4$  isotopic value of the chamber samples was compared to an ambient air sample collected at the plot before chamber closure to determine the net isotopic value using Keeling plots following calculations described by Fisher et al. (2017).

### 2.3. Analysis of Porewater Chemistry and Emitted Isotopes

Paired porewater  $\delta^{13}\text{C-CH}_4$  and  $\delta^{13}\text{C-CO}_2$  values and headspace  $\text{CH}_4$  and  $\text{CO}_2$  concentrations were analyzed at Florida State University (FSU), via a continuous-flow Hewlett-Packard 5890 gas chromatograph (Agilent Technologies) with a column temperature of  $40^\circ\text{C}$  coupled to a Finnigan MAT Delta isotope ratio mass spectrometer (GC-IRMS) via a ConFlo IV interface system (Thermo Scientific) (Hodgkins et al., 2015). Headspace concentrations were converted to dissolved forms based on headspace-to-water volume ratios and the proportion of formerly dissolved gas in the headspace after acidification (“extraction efficiency”; Corbett et al., 2013; Hodgkins, 2016). We used an extraction efficiency of 0.95 for  $\text{CH}_4$  while total dissolved inorganic carbon ( $\sum\text{CO}_2$ ) extraction efficiency was determined based on dissolved bicarbonate standards (Hodgkins, 2016). Porewater  $\text{CO}_2$  concentrations represent  $\sum\text{CO}_2$  but are herein referred to as  $\text{CO}_2$ . Methane concentrations from the chamber headspace (emitted fluxes) were determined via analysis with a gas chromatograph equipped with a flame ionization detector (GC-FID, Shimadzu GC-14A) at the University of New Hampshire (UNH) following Treat et al. (2007). Paired porewater  $\delta^{13}\text{C-CH}_4$  and  $\delta\text{D-CH}_4$  were determined using an Aerodyne dual Tunable Infrared Laser Direct Absorption Spectroscopy (TILDAS) at UNH as described by Perryman et al. (2022) and Robison et al. (2022). Porewater  $\delta^{13}\text{C-CH}_4$  values from Abisko were only run at UNH. A previous comparison of  $\delta^{13}\text{C-CH}_4$  values from the same samples between FSU (GC-IRMS) and UNH (TILDAS) analytical methods were highly correlated (linear regression,  $r^2 = 0.80$ ,  $P < 0.0001$ ,  $n = 64$ ; Bennett, 2020). The  $\delta^{13}\text{C-CH}_4$  of chamber headspace and ambient air samples used to calculate emitted  $\delta^{13}\text{C-CH}_4$  were also determined via TILDAS following Perryman et al. (2023).

We used the paired  $\delta^{13}\text{C-CH}_4$  and  $\delta^{13}\text{C-CO}_2$  to calculate apparent fractionation factors ( $\alpha\text{C}$ ; Equation 1) to further distinguish  $\text{CH}_4$  production pathways by accounting for the co-production (acetoclastic methanogenesis) or utilization (hydrogenotrophic methanogenesis) of  $\text{CO}_2$  following the methods used by Hodgkins et al. (2014) based on Whiticar et al. (1986), wherein  $\alpha\text{C}$  is calculated as follows:

$$\alpha\text{C} = (\delta^{13}\text{C} - \text{CO}_2 + 1,000) / (\delta^{13}\text{C} - \text{CH}_4 + 1,000) \quad (1)$$

### 2.4. Scaling and Sensitivity Analysis

To estimate current and potential future atmospheric  $\delta^{13}\text{C-CH}_4$  values from northern peatlands, we applied the measured fluxes and their  $\delta^{13}\text{C-CH}_4$  values from each peatland type to their respective areas in BAWLD (Olefeldt et al., 2021a, 2021b). Notably, the BAWLD land cover classification includes a fourth wetland type, tundra wetlands, which are similar in function, vegetation, and water table depth to fens, but are underlain by permafrost and can have less than 40 cm of peat (Olefeldt et al., 2021a, 2021b). For the sensitivity analysis, we applied fen fluxes and  $\delta^{13}\text{C-CH}_4$  values from this study to tundra wetlands. We determined the atmospheric  $\delta^{13}\text{C-CH}_4$  value under two time frames with differing flux magnitudes- July and the growing season (~June-August). July estimates incorporate fluxes measured in this study while growing season estimates incorporate the average growing season flux for each peatland type as synthesized by Kuhn et al. (2021). We kept  $\delta^{13}\text{C-CH}_4$  values constant across the season to test the role of landcover change. A handful of site-level studies have, however, shown that  $\delta^{13}\text{C-CH}_4$  values can vary across the growing season (e.g., McCalley et al., 2014; Throckmorton et al., 2015), but no consistent seasonal patterns have been observed yet. Thus, any potential changes between July and growing season results in our study reflect the magnitude of  $\text{CH}_4$  emissions and not changes in isotopic values.

We calculated the current northern peatland emitted isotopic values by first multiplying  $\text{CH}_4$  flux magnitudes by associated peatland areas and dividing this output for each peatland type by total peatland emissions to determine the proportion of  $\text{CH}_4$  in the atmosphere from each peatland type (Equation 2). Peatland types were split into bogs (permafrost bogs and non-permafrost bogs) and fens. We then multiplied the  $\delta^{13}\text{C-CH}_4$  values by these proportions to arrive at a mixed atmospheric value (Equation 3):

$$R = (F_{\text{PeatType}} \times A_{\text{PeatType}}) / \text{Total}_{\text{em}} \quad (2)$$

$$\text{Atm } \delta^{13}\text{C} - \text{CH}_4 = (((\delta^{13}\text{C} - \text{CH}_{4(\text{bogs})} \times R_{\text{bogs}}) + (\delta^{13}\text{C} - \text{CH}_{4(\text{fens})} \times R_{\text{fens}}))) / 100 \quad (3)$$

where  $R$  is the emission ratio for each peatland type,  $F_{\text{PeatType}}$  is the measured daily flux for each peatland type ( $\text{mg CH}_4 \text{ m}^{-2} \text{ d}^{-1}$ ),  $A_{\text{PeatType}}$  is the area of each peatland type ( $\text{m}^2$ ; determined by Olefeldt et al., 2021a, 2021b),

and  $\text{Total}_{\text{em}}$  is total  $\text{CH}_4$  emissions from peatlands ( $\text{mg CH}_4 \text{ d}^{-1}$ ).  $\text{Atm } \delta^{13}\text{C-CH}_4$  is the mixed peatland isotopic value in the atmosphere.  $\delta^{13}\text{C-CH}_4$  (bogs) and  $\delta^{13}\text{C-CH}_4$  (fens) were determined by first averaging replicates from individual plots then, by averaging values across all bog and fen plots, respectively. Uncertainty of the atmospheric mixed value was calculated using the 95% confidence intervals for the  $\delta^{13}\text{C-CH}_4$  values.

To test the influence of permafrost thaw and potential shifts in landscape wetting and drying on growing season peatland atmospheric values, we ran a sensitivity analysis looking at shifts in peatland type areas and sedge cover. We altered the areas of the peatland types in BAWLD to reflect potential landcover transitions driven by warmer temperatures and permafrost thaw. Warming and permafrost thaw can lead to a wetter landscape through the thawing and subsequent karsting of ice-rich permafrost causing wetland expansion (Turetsky et al., 2020). Further, glacial meltwater contributions can also lead to wetland expansion (Turetsky et al., 2020). In our landscape thawing and wetting scenarios, raised permafrost bogs thaw and are converted to tundra wetlands and fens. Alternatively, permafrost thaw can lead to a drier landscape through the draining of tundra wetlands underlain by permafrost, transitioning the ecosystem to drier, bog-like peatlands (Lawrence et al., 2015). Climate change can also lead to more evaporation and less precipitation, lowering water tables, and shifting vegetation communities (Zhang et al., 2020), leading fens to act more functionally like bogs. Thus, in our landscape thawing and drying scenarios, permafrost bogs, tundra wetlands, and fens are converted to bogs (see Table S5 and Figure S7 in Supporting Information S1).

We ran the sensitivity test with five peatland area scenarios including; no change in current areas, 10% and 20% drier, and 10% and 20% wetter peatland landscapes (Table S3, Figure S3 in Supporting Information S1). Within each of the change in area scenarios, we also assessed the sensitivity of porewater  $\delta^{13}\text{C-CH}_4$  values to changes in sedge cover using a linear mixed effects model (see below) with the interactive effects of peatland type and sedge cover ( $\pm 20\%$ , 40%, 60%, 80% change in relative sedge cover; Tables S4 and S5 in Supporting Information S1). While this model was not the highest-performing model it represents the best- model with predictor variables that can be remotely sensed (Table S6 in Supporting Information S1). We then used the modeled porewater  $\delta^{13}\text{C-CH}_4$  values to predict emitted values based on a linear relationship between porewater values and emitted values. Notably, these scenarios serve as a sensitivity analysis to test the effects of potential shifts in peatland types and sedge cover on  $\delta^{13}\text{C-CH}_4$  values and do not represent modeled/predicted land cover changes (Figure S9 in Supporting Information S1).

## 2.5. Statistical Analysis

All statistical analyses were performed in R statistical software (R Core Team, 2023). Statistical tests were performed using linear mixed-effects models (R Package 3.3.3; Lme4 Package (Bates, 2010)). We included random effects of the individual plots and circumpolar location to account for multiple sampling depths per plot and nested variation within the five locations, respectively. Each linear mixed-effect model was compared to the respective null model, which only included the random effects, using an ANOVA (“anova” command) to test for significance (significance level = 0.05). If significant, individual peatland type pairs were then compared using a post-hoc, parametric *t*-test (Tukey's adjustment). Model performance for predicting porewater  $\delta^{13}\text{C-CH}_4$  was conducted using size-corrected Akaike information criterion (AICc; “AICcmodavg” package; Mazerolle & Mazerolle, 2017). All data and model residuals followed approximate normal distributions. Results are presented as mean  $\pm$  standard deviations unless otherwise noted.

## 3. Results

Our multi-site data set of porewater chemistry shows large variations and differences in stable  $\text{CH}_4$  isotope values among peatland types, indicating different  $\text{CH}_4$  production pathways. Dissolved porewater  $\text{CH}_4$  concentrations ranged between 0.01 and 1.32 mM and did not differ across peatland types ( $P = 0.28$ , Figure 2a;  $n = 291$ ; Tables S7 and S8 in Supporting Information S1) or by peatland type interacting with depth ( $P = 0.4$ ; Figure 2a). Porewater  $\delta^{13}\text{C-CH}_4$  ranged from  $-99.9\text{‰}$  to  $-35.9\text{‰}$  and was  $\delta^{13}\text{C}$  enriched in fens (mean  $\pm$  standard deviation;  $-62.9 \pm 9.4\text{‰}$ ) compared to bogs ( $-74.1 \pm 9.3\text{‰}$ ) and permafrost bogs ( $-81.6 \pm 11.5\text{‰}$ ,  $P < 0.001$ ;  $n = 291$ ; Figure 2b), indicating a potentially greater importance of acetoclastic methanogenesis (potential oxidation effects withstanding) in fens than in bogs. This pattern held when we included values from the literature ( $P < 0.001$ ,  $n = 43$ ; Figure 3).

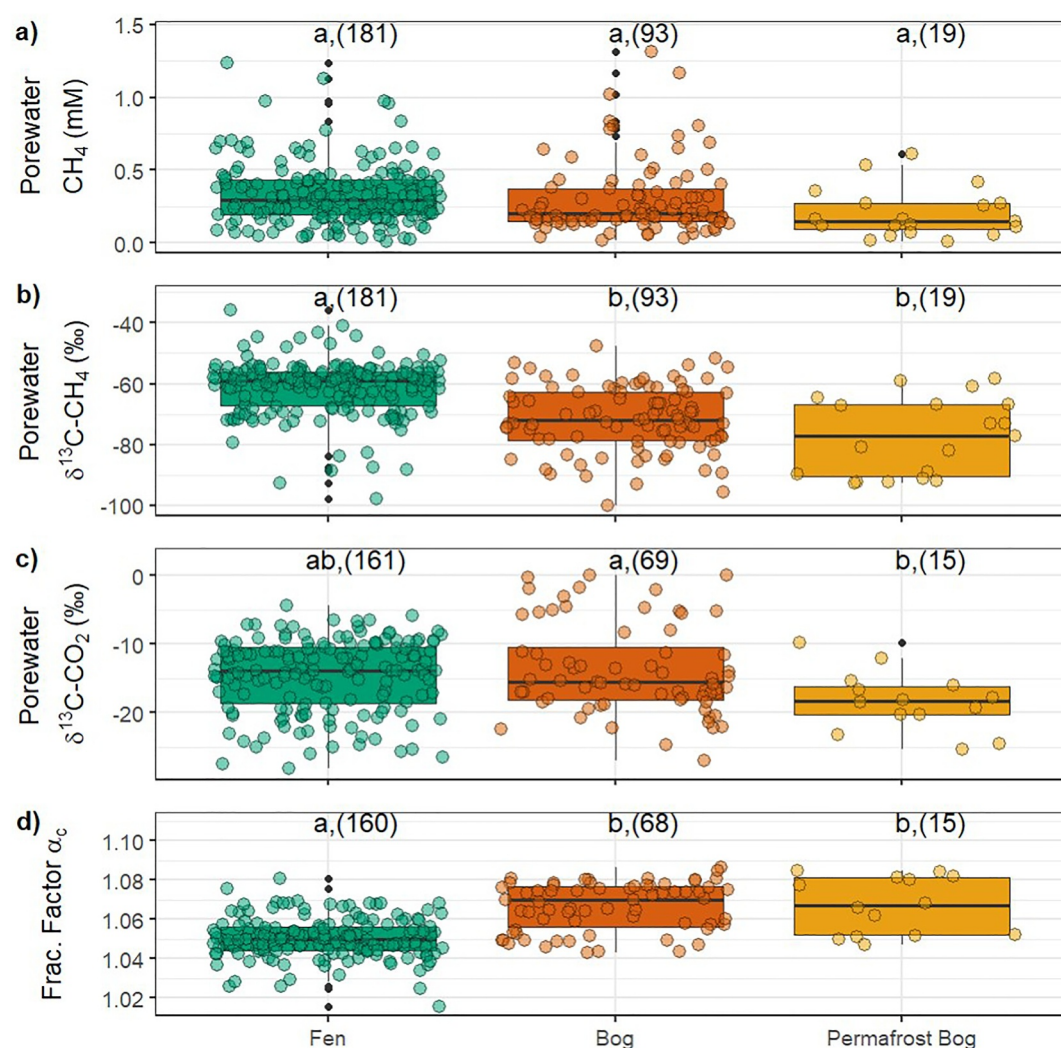


**Figure 2.** Porewater chemistry across peatland types from all five locations including (a) dissolved CH<sub>4</sub>, (b) δ<sup>13</sup>C-CH<sub>4</sub>, (c) δ<sup>13</sup>C-CO<sub>2</sub>, and (d) the fractionation factor (α<sub>c</sub>), defined as (δ<sup>13</sup>C-CO<sub>2</sub> + 1,000)/(δ<sup>13</sup>C-CH<sub>4</sub> + 1,000). Colored points represent individual measurements across multiple plots at depths between 0 and 60 cm. Statistical differences (denoted by the letters) were determined using mixed linear regression with individual plots and circumpolar location as random factors to account for multiple samples at each depth and plot and natural variation within the location (significance level 5%; Tukey's HSD:  $P < 0.05$ ). When letters differ between boxes in each row this indicates significant differences. Boxes show 25th to 75th percentiles. Whiskers indicate 10th and 90th percentiles and black points outliers. Horizontal lines denote medians. Sample sizes are indicated next to the letters.

For the subset of samples ( $n = 193$ ) used to determine the best predictive model for porewater δ<sup>13</sup>C-CH<sub>4</sub>, peatland type explained 27% of the variation in porewater δ<sup>13</sup>C-CH<sub>4</sub> ( $P < 0.001$ ) and was the best individual predictor variable (Table S6 in Supporting Information S1). Sampling depth was not a significant predictor variable on its own ( $P = 0.3$ ; Table S6 in Supporting Information S1), nor while interacting with peatland type ( $P = 0.21$ ; Table S6 in Supporting Information S1). Within all peatland types, porewater δ<sup>13</sup>C-CH<sub>4</sub> was positively correlated with pH ( $r^2 = 0.21$ ,  $P < 0.0013$ ) and percent sedge cover ( $r^2 = 0.14$ ,  $P < 0.001$ ; Figure S4 in Supporting Information S1). The interactive effects of sedge cover and peatland type and pH and peatland type explained 35% and 44% of the variation, respectively ( $P < 0.001$ , each). Porewater CH<sub>4</sub> concentration on its own only explained 4% of the variation in porewater δ<sup>13</sup>C-CH<sub>4</sub> ( $P < 0.001$ ); however, a combination of porewater CH<sub>4</sub>, sedge cover, and the interactive effect of peatland type and pH explained half the variation in δ<sup>13</sup>C-CH<sub>4</sub> ( $r^2 = 0.50$ ,  $P < 0.001$ ) and was the best performing model (AIC analysis; Table S6 in Supporting Information S1).



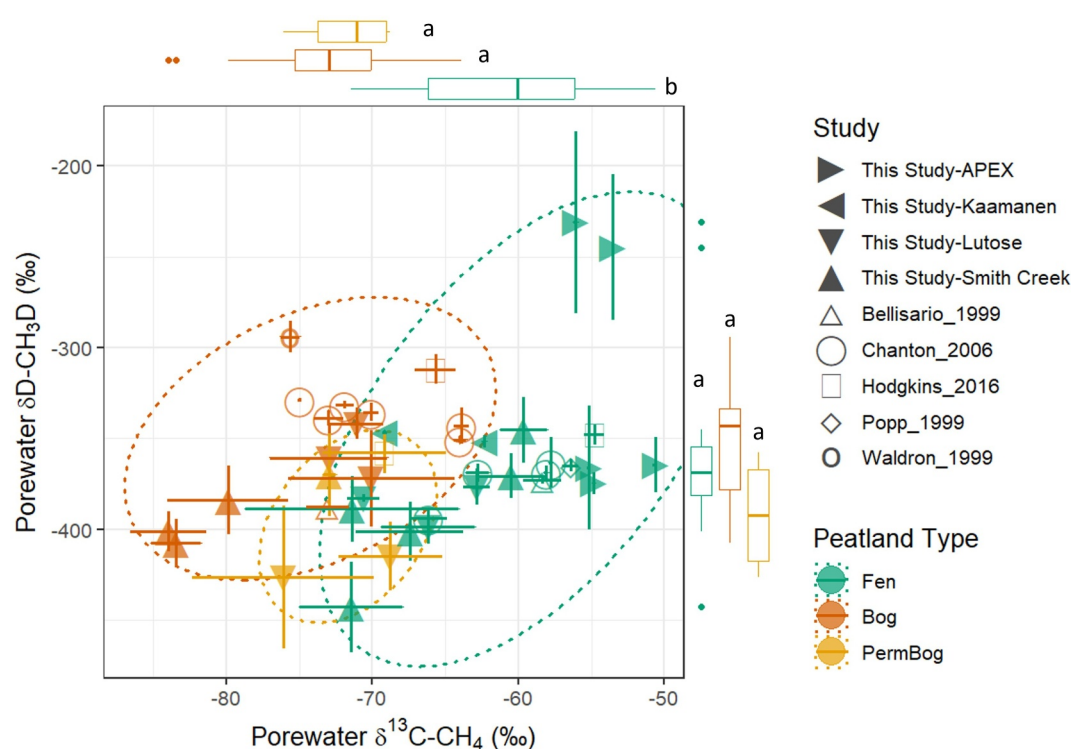


**Figure 3.** Relationships of  $\delta^{13}\text{C-CH}_4$  and  $\delta\text{D-CH}_4$  in a subset of peat porewater samples for different types of peatlands across four of the locations sampled in this study ( $\delta\text{D-CH}_4$  samples were not taken at Abisko) compared to peatland values from other studies (open shapes). The symbols are plot-specific means, and error bars denote standard error for individual peatland types in each location. “PermBog” = Permafrost Bog. The ellipses represent the 95% confidence interval. Boxplots on the x and y axes show the distribution of  $\delta^{13}\text{C-CH}_4$  and  $\delta\text{D-CH}_4$  by peatland type, respectively.

Porewater  $\text{CO}_2$  concentrations varied between 0.6 and 11.4 mM. Concentrations were similar across the peatland types, with an exception for bogs, which had slightly lower concentrations ( $2.25 \pm 1.34$ ) compared to fens ( $3.79 \pm 2.00$ ,  $P < 0.01$ ), but similar concentrations to permafrost bogs ( $2.25 \pm 1.34$ ,  $P = 0.54$ ,  $n = 242$ ; Figure S5 in Supporting Information S1). Porewater  $\delta^{13}\text{C-CO}_2$  values ranged from  $-28.2$  to  $0.02\text{‰}$  (average =  $-14.5 \pm 4.6\text{‰}$ ) and were statistically more similar across the peatland types with minor difference between permafrost bogs and bogs ( $P = 0.03$ ,  $n = 242$ ; Figure 2c).

The apparent fractionation factor ( $\alpha_C$ ), which further distinguishes  $\text{CH}_4$  production pathways by accounting for the co-production (acetoclastic methanogenesis; lower  $\alpha_C$ ) and/or utilization (hydrogenotrophic methanogenesis; higher  $\alpha_C$ ) of  $\text{CO}_2$  (Hodgkins et al., 2015; Whiticar et al., 1986), followed similar patterns to  $\delta^{13}\text{C-CH}_4$ , with higher  $\alpha_C$  values in permafrost bogs and bogs (1.07, each) and lower values in fens (1.05,  $P < 0.001$ ,  $n = 240$ ; Figure 2d).  $\delta\text{D-CH}_4$  varied from  $-442.9\text{‰}$  to  $-231.0\text{‰}$  ( $n = 25$ ; Figure 3). The greatest change in  $\delta\text{D-CH}_4$  was between 10 and 30 cm below the peat surface for two fens at the APEX site ( $\sim -250$  and  $-375\text{‰}$ , respectively; Figure S6 in Supporting Information S1). However, we found no significant differences between peatland types in our study ( $P = 0.44$ ,  $n = 24$ ; Figure 3 and Figure S5 in Supporting Information S1) or those in the literature ( $P = 0.14$ ,  $n = 43$ ; Figure 3), nor did we find a significant relationship with depth ( $P = 0.50$ ,  $n = 24$ ).

Average emitted  $\delta^{13}\text{C-CH}_4$  fluxes varied between  $-85.6\text{‰}$  and  $-46.7\text{‰}$  (mean  $\pm$  95% CI of plot averages =  $-67.9 \pm 7.3\text{‰}$ ) and differed between fens and permafrost bogs/bogs ( $P = 0.01$ ,  $n = 10$ ). Emitted  $\delta^{13}\text{C-CH}_4$  fluxes closely correlated with average porewater  $\delta^{13}\text{C-CH}_4$  for those respective sites ( $r^2 = 0.60$ ,  $P = 0.008$ ,  $n = 11$ ; Figure 4). Methane fluxes ranged from 1 to 617  $\text{mg CH}_4 \text{ m}^{-2} \text{ d}^{-1}$  with the greater fluxes from fens ( $253.0 \pm 220 \text{ mg CH}_4 \text{ m}^{-2} \text{ d}^{-1}$ ;  $n = 6$ ) than from bogs ( $87.3 \pm 81.6 \text{ mg CH}_4 \text{ m}^{-2} \text{ d}^{-1}$ ;  $n = 4$ ) and permafrost bogs ( $2.2 \pm 1.0 \text{ mg CH}_4 \text{ m}^{-2} \text{ d}^{-1}$ ;  $n = 2$ ; Figure S7 in Supporting Information S1). Due to a small sample size, we did not perform statistical analysis between peatland types.

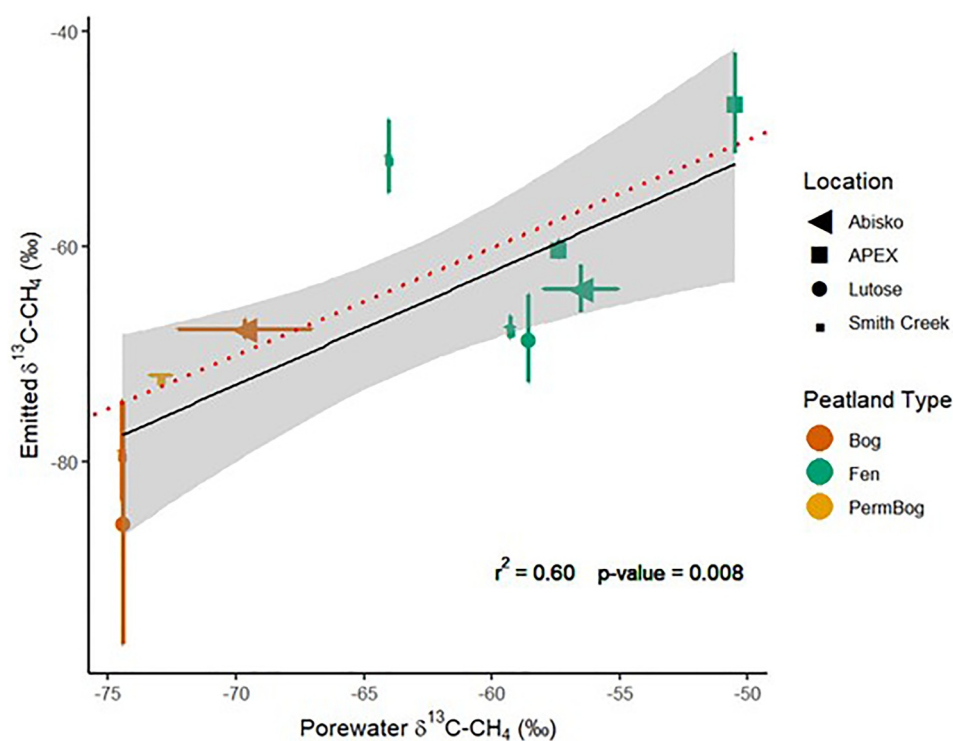


**Figure 4.** Relationship between below-ground and emitted  $\delta^{13}\text{C-CH}_4$ . The red dotted line represents the 1:1 line while the black line represents the regression slope. Points represent average emitted fluxes from individual plots (y-axis) or the average value across all porewater depths at that plot (x-axis). Kaamanen data was not included here due to limited samples and high instrument error for emitted isotopes. “Permbog” = permafrost bog. The sampling depths ranged from 10 to 50 cm for fens, 10–60 cm for bogs, and 10–30 cm for the Smith Creek permafrost bog.

When accounting for differences in area, flux magnitude, and emitted isotopic values for fens and bogs, mixed atmospheric peatland values for July and growing season were  $-63.6 \pm 7\text{‰}$  and  $-65.3 \pm 7\text{‰}$ , respectively (simple scaling; Figure 5). The modeled growing season value, which accounted for the average sedge cover in each peatland type, was more depleted than the simple scaling estimate by  $1.4\text{‰}$  (Figure 5). Under the sensitivity analysis scenarios, the mixed atmospheric value of peatland  $\text{CH}_4$  became enriched when fen area and sedge cover increased, with value changes of  $0.7\text{--}3.5\text{‰}$  under  $10\text{--}20\%$  wetter scenarios (Figure 5). However, values changed more under the drying scenarios wherein the landscape shifted toward more bogs with less sedge cover, depleting values by  $1.1\text{--}5.7\text{‰}$  ( $10\text{--}20\%$  drier scenarios; Figure 5). The atmospheric value was highly sensitive to changes in sedge cover and changed the current peatland area atmospheric value  $5.3\text{‰}$  ( $64.1\text{--}69.4\text{‰}$ ) when relative sedge cover was changed between  $-80$  and  $+80\%$  for each peatland type.

## 4. Discussion

### 4.1. Drivers of Peatland Porewater $\delta^{13}\text{C-CH}_4$ Values

Analysis of our multi-site data set of 240 porewater samples showed that  $\delta^{13}\text{C-CH}_4$  and  $\alpha_C$  values correlate with peatland types across the five northern locations. We found that porewater  $\delta^{13}\text{C-CH}_4$  differs significantly between fens and bogs/permafrost bogs (Figure 2), which is in line with results from previous northern peatland studies (Blaser & Conrad, 2016; Chanton et al., 2006; Corbett et al., 2015; Heffernan et al., 2022; Hodgkins et al., 2014; Hornibrook, 2009; McCalley et al., 2014; Whiticar, 1999). Fens in our study had a mean porewater  $\delta^{13}\text{C-CH}_4$  value ( $-61.2\text{‰}$ ) that fell within the expected range of acetoclastic methanogenesis ( $-70$  to  $-30\text{‰}$ ), while permafrost bogs and bogs (herein referred to as bogs) had mean porewater values ( $-74.1\text{‰}$  and  $-81.5\text{‰}$ , respectively) falling within the expected range of hydrogenotrophic methanogenesis ( $-100$  to  $-60\text{‰}$ ; Figure 2).

Differences in apparent  $\text{CH}_4$  production pathways between fens and bogs were further supported by  $\alpha_C$  values (Figure 2), with larger isotopic fractionation between  $\text{CO}_2$  and  $\text{CH}_4$  in bogs indicating higher contribution of

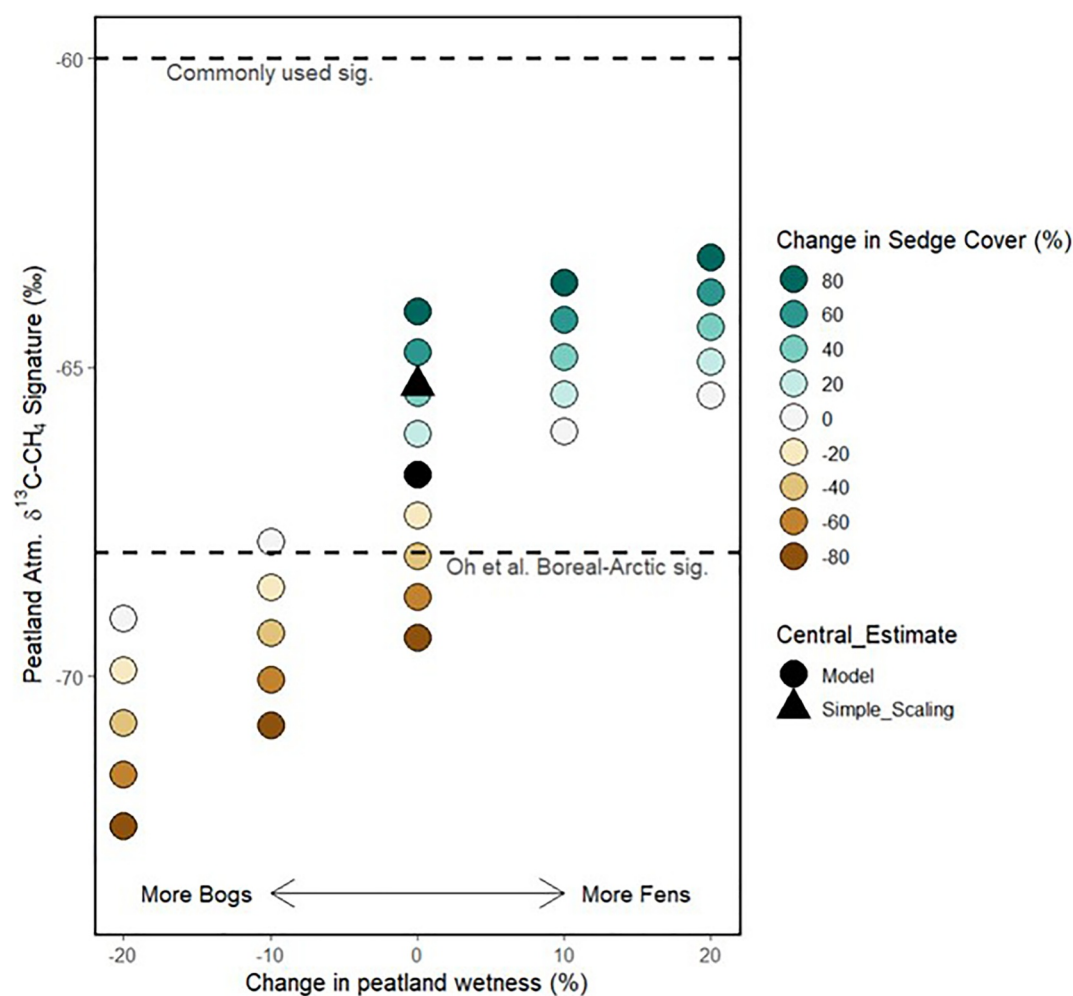


**Figure 5.** Sensitivity analysis of atmospheric growing season peatland  $\delta^{13}\text{C-CH}_4$  values to potential shifts in peatland type areas and sedge cover. Zero changes in sedge cover and wetness represent the current peatland types, determined by vegetation surveys in this study. The increases and decreases in peatland wetness represent potential shifts in bogs versus fen areas (see also Figure S9 in Supporting Information S1). Estimates of current peatland  $\delta^{13}\text{C-CH}_4$  values are represented by black points. Circles represent the output from the mixed model and the triangle represents the output from the simple, means-weighted scaling approach. On the  $x$ -axis, positive values represent a potential shift toward more fens while negative values represent a shift toward more bogs. Colors represent relative changes in sedge cover respective to each peatland type. The dotted lines represent the commonly used, simplified isotopic signature (i.e. value) for northern peatlands ( $-60\text{‰}$ ) and the suggested signature for the boreal-Arctic region (Oh et al., 2022; Ganesan et al., 2018;  $-68\text{‰}$ ). Peatland areas are from Olefeldt et al. (2021a, 2021b).

hydrogenotrophic methanogenesis than in fens. Our  $\alpha_c$  values fall within the previously established ranges reported across a latitudinal transect in Alaska (Chanton et al., 2006), and previously reported values for sites in this study, including at Lutose, Alberta (Heffernan et al., 2022) and Abisko, Sweden (Stordalen Mire; Hodgkins et al., 2014) (Table S9 in Supporting Information S1), which matches findings from previous studies (Galand et al., 2010; Keller & Bridgham, 2007; Kelly et al., 1992). While earlier studies highlighted the increasingly dominant role of hydrogenotrophic methanogenesis with depth in the peat profile (Chasar et al., 2000; Hornibrook et al., 1997), here peatland type explained more variation in  $\delta^{13}\text{C-CH}_4$  than sampling depth, which on its own was a non-significant predictor (Table S6 in Supporting Information S1). It's possible that our sampling design did not capture a large enough depth gradient to see shifts to hydrogenotrophic production. For example, we only sampled 10–60 cm below the surface and some sites have peat depths greater than 200 cm (Lutose; Heffernan et al., 2022), similar to depth profiles in Chasar et al. (2000) and Hornibrook et al. (1997).

Peatland type was the best individual predictor of porewater  $\delta^{13}\text{C-CH}_4$ , but pH, sedge cover, and porewater  $\text{CH}_4$  improved model performance ( $r^2 = 0.50$ ). Our results are in line with previous studies that found that nutrient-rich wetlands with more vascular plants and higher pH stimulate the production of labile organic substrates for acetoclastic methanogenesis, which would be more prevalent in fens (Heffernan et al., 2022; Hines et al., 2008; Hodgkins et al., 2014; McCalley et al., 2014). Notably, the interactive effects of pH and peatland type explained even more variation (44%) in porewater  $\delta^{13}\text{C-CH}_4$  than peatland type alone, reflecting the range of pH conditions within peatland types and the potential impact on  $\text{CH}_4$  cycling. While the connection between pH and  $\text{CH}_4$  production is complex (Conrad, 2020), the positive relationship between pH and  $\delta^{13}\text{C-CH}_4$  in our study could suggest inhibitory effects of low pH on acetoclastic methanogenesis. Similar observations have been linked to both the pooling of and the poor dissociation of acetate in low pH conditions (Hines et al., 2008; Lansdown et al., 1992), the absence of acid-tolerant acetoclastic methanogens (Horn et al., 2003), and the correlation between low pH and the presence of decomposition-inhibiting phenolic compounds (Tahvanainen & Haraguchi, 2013).

While our results demonstrate the potential for porewater pH to predict  $\delta^{13}\text{C-CH}_4$ , it is difficult to extrapolate below-ground measurements across large areas. When we only consider models that include parameters that can be remotely sensed or mapped at region scales, peatland type and sedge cover were the best predictors of porewater  $\delta^{13}\text{C-CH}_4$  (interactive effect;  $r^2 = 0.38$ ). Previous scaling efforts have used soil pH and soil organic carbon maps to predict  $\delta^{13}\text{C-CH}_4$  values (Ganesan et al., 2018; Oh et al., 2022), but often these maps are low in resolution (e.g., 30 arc seconds to 0.5 by 0.5°) and are based on limited or highly localized field samples (Chen et al., 2022), inadequately capturing the high variability in soil conditions (Hugelius et al., 2020). Given peatlands can vary at meter scales, above-ground approaches to scaling may be more reliable. As remote-sensing products increase in resolution (Bartsch et al., 2023), our results suggest that using above-ground metrics of peatland type and sedge cover to model peatland  $\delta^{13}\text{C-CH}_4$  could be a viable alternative to using pH and soil carbon-based mapping products.

#### 4.2. Effect of Oxidation and Intra-Site Comparisons of Methane Isotopes

There was little evidence that  $\text{CH}_4$  oxidation led to the observed separation in  $\delta^{13}\text{C-CH}_4$  between peatland types, as indicated by the lack of porewater samples that are enriched in both  $\delta^{13}\text{C-CH}_4$  and  $\delta\text{D-CH}_4$  (top right quadrant on Figure 3; Chanton et al., 2005). Although higher water tables and lower redox conditions have been linked to higher  $\text{CH}_4$  oxidation rates in saturated fens in subarctic Sweden (Perryman et al., 2020), these isotopic oxidation effects did not appear to separate the different peatland types (Figure 3). Apart from two fens in APEX, Alaska,  $\delta\text{D-CH}_4$  values for all peatland plots were within the same range ( $\sim -450$  to  $-350\text{‰}$ ). The two APEX plots had enriched  $\delta\text{D-CH}_4$  values towards the surface ( $-375\text{‰}$  at 30 cm to  $-230\text{‰}$  at 10 cm; Figure S8 in Supporting Information S1), suggesting an oxidation effect. A sedge rhizosphere oxidation effect has been demonstrated in mesocosms representative of the APEX site (Rupp et al., 2019), which supports sedge cover as being a significant driver of  $\delta\text{D-CH}_4$  and  $\delta^{13}\text{C-CH}_4$  enrichment in the APEX fens included in this study.

A comparison of porewater  $\delta^{13}\text{C-CH}_4$  and  $\delta\text{D-CH}_4$  signatures in our study and those reported in the literature (Bellisario et al., 1999; Chanton et al., 2006; Hodgkins, 2016; Popp et al., 1999; Waldron, Hall, & Fallick, 1999; Waldron, Lansdown, et al., 1999), suggests that  $\delta^{13}\text{C-CH}_4$  can be used effectively to distinguish between bogs and fens, due to the strong role of methanogenesis pathway in shifting  $\delta^{13}\text{C}$  signatures ( $P < 0.001$ ; Figure 3). In contrast, there appears to be little distinction in  $\delta\text{D-CH}_4$  between peatland types ( $P = 0.14$ ) in our study. While  $\delta\text{D-CH}_4$  signatures can be indicative of differences in  $\text{CH}_4$  production pathways (Chanton et al., 2005; Whiticar, 1999; Whiticar et al., 1986),  $\delta\text{D-CH}_4$  is also impacted by other factors including latitudinal or evaporative changes in  $\delta\text{D}$  of water, a hydrogen precursor to the hydrogen in methane (Chanton et al., 2006; Douglas et al., 2021; Waldron, Hall, & Fallick, 1999; Waldron, Lansdown, et al., 1999), and also the concentration of di-hydrogen in the soils (Burke, 1993). Waldron, Hall, and Fallick (1999) and Waldron, Lansdown, et al. (1999), suggested that some of the justification for the observation that the  $\delta\text{D}$  of  $\text{CH}_4$  was a good indicator of the difference between acetate-formed  $\text{CH}_4$  versus  $\text{CO}_2$  reduction  $\text{CH}_4$  is because  $\text{CH}_4$  samples that were representative of the  $\text{CO}_2$  reduction pathway were often from the marine environment where the  $\delta\text{D-H}_2\text{O}$  is close to 0‰, the signature of ocean water. Methane representative of acetate fermentation was more likely sampled from terrestrial environments where the  $\delta\text{D-H}_2\text{O}$  was depleted relative to marine  $\text{H}_2\text{O}$  (Waldron, Hall, & Fallick, 1999; Waldron, Lansdown, et al., 1999). For terrestrial environments at high latitudes, the effect would be even more pronounced (Waldron, Hall, &

Fallick, 1999; Waldron, Lansdown, et al., 1999). Thus in our opinion, for these reasons,  $\delta\text{D-CH}_4$  is a less reliable indicator of pathway and wetland type than  $\delta^{13}\text{C-CH}_4$ .

Interestingly, our observed patterns in peatland  $\text{CH}_4$  isotopes differed from intra-site comparisons of isotopes from northern lake  $\text{CH}_4$  bubbles. Wik et al. (2020) found that the  $\text{CH}_4$  isotopes in bubbles from distinct lake types (thermokarst, peatland, glacial/post-glacial) were separated based on  $\delta\text{D-CH}_4$  but not based on  $\delta^{13}\text{C-CH}_4$ . Douglas et al. similarly found that  $\delta\text{D-CH}_4$  varied more than  $\delta^{13}\text{C-CH}_4$  in high-latitude inland waters, opposite of wetlands, potentially driven by variable and potentially more dominant oxidation in inland waters (2021). Further, the range of  $\delta^{13}\text{C-CH}_4$  values from lake bubbles ( $\sim -80$  to  $-50\%$ ) overlaps with peatland porewater  $\delta^{13}\text{C-CH}_4$  values in our study ( $-99.9\%$  to  $-35.9\%$ ). These results indicate that while  $\delta^{13}\text{C-CH}_4$  can potentially be used to distinguish between peatland types, it may be harder to confidently separate peatland and lake emissions in northern regions.

#### 4.3. Emitted Isotope Patterns and Atmospheric Values

We found a positive relationship between porewater  $\delta^{13}\text{C-CH}_4$  and emitted  $\delta^{13}\text{C-CH}_4$  ( $r^2 = 0.60$ ; Figure 4), despite having a limited sample size ( $n = 11$ ). There was no discernible evidence of consistent oxidation or plant-transport effects on emitted isotopes across peatland types as indicated by bog and fen points that fall both below and above the 1:1 line. Our findings differ from previous northern studies that observed emitted values for bogs and fens falling predominantly below the 1:1 line, indicating a fractionation effect from plant transport (Hornibrook, 2009; Marushchak et al., 2016). The differences could potentially be explained by higher rates of oxidation or less vascular plant cover in our study plots. For example, as highlighted previously,  $\delta^{13}\text{C-CH}_4$  and  $\delta\text{D-CH}_4$  values suggest oxidation is responsible for enriched  $\delta^{13}\text{C-CH}_4$  values compared to porewater values. However, only one of the two APEX fen plots is above the 1:1 line, which also suggests that plant transport can mask the signal of oxidation in emitted  $\delta^{13}\text{C-CH}_4$  values. While more measurements of emitted isotopes are required, our results suggest that emitted  $\delta^{13}\text{C-CH}_4$  values reflect below-ground patterns and have the potential to be used to predict emissions values from this region.

Our chamber measurements showed a wide range in emitted  $\delta^{13}\text{C-CH}_4$  values from fens ( $-42\%$  to  $-80.5\%$ ) and bogs ( $-72\%$  to  $-97\%$ ). It is notable that chamber-based measurements are limited by small area coverage and potential changes in isotopic value during the enclosure period due to pressure changes and ebullition (Hornibrook, 2009); thus, large spatial coverage is required to constrain uncertainty (Fisher et al., 2017). Despite the limitations of chamber measurements, emitted  $\delta^{13}\text{C-CH}_4$  differed between fens and bogs in our study ( $P < 0.01$ ). When we accounted for the area, flux magnitude, and emitted isotopic value of  $\text{CH}_4$  from fens and bogs, we found a peak season (July) atmospheric value of  $-63.6 \pm 7\%$  and a growing season value of  $-65.3 \pm 7\%$  (simple scaling approach; Figure 5). Our growing season value estimate is on the outer range of reported aircraft measurements for wetlands over northern Europe ( $-70.5 \pm 2.7\%$ ; Fisher et al., 2017), but is within the suggested  $\delta^{13}\text{C-CH}_4$  atmospheric value range for all northern peatlands ( $-68 \pm 4\%$ ; Ganesan et al., 2018; Oh et al., 2022) and is similar to reported values from aircraft measurements over Saskatchewan peatlands ( $-66.8 \pm 1.6\%$ ; Miller et al., 2014). Despite overlapping uncertainty, our average isotope values match previous studies and similarly suggest that northern peatland values are more depleted than the historically used  $-60\%$  value (Bousquet et al., 2006; Houweling et al., 2000; Mikaloff Fletcher et al., 2004; Monteil et al., 2011; Rigby et al., 2012) (Figure 5).

#### 4.4. Sensitivity of Northern Peatland $\delta^{13}\text{C-CH}_4$ Atmospheric Values to Change

Currently, fens and wet tundra are the dominant source of peatland/wetland  $\text{CH}_4$  emissions in the boreal-Arctic region (Kuhn et al., 2021), but that may change as permafrost thaws, altering the distribution of soil moisture (i.e., hydrology) and vegetation cover across peatlands. In our sensitivity analysis,  $\delta^{13}\text{C-CH}_4$  values were enriched slightly ( $0.7$ – $3.5\%$  enrichment) under the wetting scenarios wherein fen and sedge area increased. However, values changed more under the drying scenarios wherein bog area expanded and sedge cover was reduced ( $1.1$ – $5.7\%$  depletion; Figure 5). Under all scenarios, values were more depleted than the historically used wetland values of  $-60\%$ . For the wetting scenarios, modeled values were enriched ( $-66$  to  $-63\%$ ) compared to the suggested value for the boreal-Arctic region of  $-68\%$  (Ganesan et al., 2018; Oh et al., 2022). Under the drying scenarios, modeled values were near or more depleted than  $-68\%$  ( $-72.4$  to  $-67.8\%$ ; Figure 5). Notably, the sedge cover estimates used in our models are dependent on ground-based vegetation surveys; to improve

estimates of emitted  $\delta^{13}\text{C-CH}_4$  values, we need high-resolution remote sensing products to quantify sedge cover over larger areas. However, our results demonstrate that as the northern region experiences accelerated rates of permafrost thaw we are likely to see changes in the  $\delta^{13}\text{C-CH}_4$  values of northern peatlands. We suggest these changes need to be reflected in spatial  $\delta^{13}\text{C-CH}_4$  products like those developed by Oh et al. (2022) and Ganesan et al. (2018) to improve inversion model estimates of annual  $\text{CH}_4$  emissions.

## 5. Future Research Directions and Conclusions

Our results suggest broadly defined peatland types explain some of the variation in porewater  $\delta^{13}\text{C-CH}_4$ , but including variation in pH and sedge cover within the peatland types helps improve model performance. We additionally show that the atmospheric  $\delta^{13}\text{C-CH}_4$  value of northern peatlands is sensitive to thaw-driven hydrological shifts and associated changes in peatland types and sedge cover across the landscape. However, more plot-level measurements of emitted  $\delta^{13}\text{C-CH}_4$  are needed to confidently partition  $\delta^{13}\text{C-CH}_4$  values from northern peatlands and constrain the atmospheric value. Notably, our work establishes differences in  $\delta^{13}\text{C-CH}_4$  values during July only and does not cover potential changes in production pathways and values over the entire growing season or year, which could be significant (Chang et al., 2021; Marushchak et al., 2016; Throckmorton et al., 2015). Further, our study represents snapshots across single years. Annual changes in temperature and precipitation could alter observations of  $\delta^{13}\text{C-CH}_4$  and should be considered in future studies. Still, our work reinforces the need to develop models that incorporate differences in  $\delta^{13}\text{C-CH}_4$  values between and within peatland types and to also consider how climate change will impact landscape composition and thus impact  $\delta^{13}\text{C-CH}_4$  values. Here we provide evidence that peatland type and sedge cover may be valuable predictors for northern peatland  $\delta^{13}\text{C-CH}_4$  values.

## Data Availability Statement

All data are available on the EMERGE database ([https://emerge-db.asc.ohio-state.edu/datasources/0154\\_A2A\\_Summary\\_Files](https://emerge-db.asc.ohio-state.edu/datasources/0154_A2A_Summary_Files)). The Boreal-Arctic Wetland and Lake Data set (BAWLD) is available at the Arctic Data Center (<https://doi.org/10.18739/A2C824F9X>).

## References

- Åkerman, H. J., & Johansson, M. (2008). Thawing permafrost and thicker active layers in sub-arctic Sweden. *Permafrost and Periglacial Processes*, 19(3), 279–292. <https://doi.org/10.1002/ppp.626>
- Bansal, S., Creed, I. F., Tangen, B. A., Bridgman, S. D., Desai, A. R., Krauss, K. W., et al. (2023). Practical guide to measuring wetland carbon pools and fluxes. *Wetlands*, 43(8), 105. <https://doi.org/10.1007/s13157-023-01722-2>
- Bansal, S., Post van der Burg, M., Fern, R. R., Jones, J. W., Lo, R., McKenna, O. P., et al. (2023). Large increases in methane emissions expected from North America's largest wetland complex. *Science Advances*, 9(9), eade1112. <https://doi.org/10.1038/d41586-023-00616-x>
- Bartsch, A., Efimova, A., Widhalm, B., Muri, X., von Baeckmann, C., Bergstedt, H., et al. (2023). Circumarctic landcover diversity considering wetness gradients. *EGU Sphere*, 2023, 1–98. <https://doi.org/10.5194/egusphere-2023-2295>
- Basu, S., Lan, X., Dlugokencky, E., Michel, S., Schwietzke, S., Miller, J. B., et al. (2022). Estimating emissions of methane consistent with atmospheric measurements of methane and  $\delta^{13}\text{C}$  of methane. *Atmospheric Chemistry and Physics*, 22(23), 15351–15377. <https://doi.org/10.5194/acp-22-15351-2022>
- Bates, D. M. (2010). LME4 package. Retrieved from [https://www.researchgate.net/profile/Dimitris-Kavroudis/post/What\\_is\\_the\\_appropriate\\_package\\_to\\_use\\_for\\_performing\\_NML\\_using\\_R/attachment/59d62f0dc49f478072e9f5e7/AS%3A272534858076166%401441988781179/download/lrgprt.pdf](https://www.researchgate.net/profile/Dimitris-Kavroudis/post/What_is_the_appropriate_package_to_use_for_performing_NML_using_R/attachment/59d62f0dc49f478072e9f5e7/AS%3A272534858076166%401441988781179/download/lrgprt.pdf)
- Bellisario, L. M., Bubier, J. L., Moore, T. R., & Chanton, J. P. (1999). Controls on  $\text{CH}_4$  emissions from a northern peatland. *Global Biogeochemical Cycles*, 13(1), 81–91. <https://doi.org/10.1029/1998gb900021>
- Bennett, K. (2020). *Using stable isotopes to determine dominant methane production pathways of thaw ponds in a subarctic peatland* (Master's Thesis). University of New Hampshire. Retrieved from <https://scholars.unh.edu/thesis/1414>
- Blaser, M., & Conrad, R. (2016). Stable carbon isotope fractionation as tracer of carbon cycling in anoxic soil ecosystems. *Current Opinion in Biotechnology*, 41, 122–129. <https://doi.org/10.1016/j.copbio.2016.07.001>
- Bloom, A. A., Bowman, K. W., Lee, M., Turner, A. J., Schroeder, R., Worden, J. R., et al. (2017). A global wetland methane emissions and uncertainty dataset for atmospheric chemical transport models (WetCHARTs version 1.0). *Geoscientific Model Development*, 10(6), 2141–2156. <https://doi.org/10.5194/gmd-10-2141-2017>
- Bousquet, P., Ciais, P., Miller, J. B., Dlugokencky, E. J., Hauglustaine, D. A., Prigent, C., et al. (2006). Contribution of anthropogenic and natural sources to atmospheric methane variability. *Nature*, 443(7110), 439–443. <https://doi.org/10.1038/nature05132>
- Brown, J., Ferrians, O., Heginbottom, J. A., & Melnikov, E. (2002). Circum-Arctic map of permafrost and ground-ice conditions, version 2 [Dataset]. *National Snow and Ice Data Center*. <https://doi.org/10.7265/skbg-kf16>
- Brownlow, R., Lowry, D., Fisher, R. E., France, J. L., Lanoisellé, M., White, B., et al. (2017). Isotopic ratios of tropical methane emissions by atmospheric measurement. *Global Biogeochemical Cycles*, 31(9), 1408–1419. <https://doi.org/10.1002/2017GB005689>
- Bruhwiller, L., Parmentier, F. J. W., Crill, P., Leonard, M., & Palmer, P. I. (2021). The Arctic carbon cycle and its response to changing climate. *Current Climate Change Reports*, 7(1), 14–34. <https://doi.org/10.1007/s40641-020-00169-5>
- Burke, R. A. (1993). Possible influence of hydrogen concentration on microbial methane stable hydrogen isotopic composition. *Chemosphere*, 26(1–4), 55–67. [https://doi.org/10.1016/0045-6535\(93\)90412-X](https://doi.org/10.1016/0045-6535(93)90412-X)

- Chang, K. Y., Riley, W. J., Knox, S. H., Jackson, R. B., McNicol, G., Poulter, B., et al. (2021). Substantial hysteresis in emergent temperature sensitivity of global wetland CH<sub>4</sub> emissions. *Nature Communications*, 12(1), 2266. <https://doi.org/10.1038/s41467-021-22452-1>
- Chanton, J. P., Chaser, L., Glasser, P., & Siegel, D. (2005). Carbon and hydrogen isotopic effects in microbial methane from terrestrial environments. *Stable Isotopes and Biosphere-Atmosphere Interactions* (pp. 85–105). Retrieved from [http://eebweb.arizona.edu/faculty/saleska/Ecol596V/Readings/Chanton.04\\_Methane\\_Ch.6.pdf](http://eebweb.arizona.edu/faculty/saleska/Ecol596V/Readings/Chanton.04_Methane_Ch.6.pdf)
- Chanton, J. P., Fields, D., & Hines, M. E. (2006). Controls on the hydrogen isotopic composition of biogenic methane from high-latitude terrestrial wetlands. *Journal of Geophysical Research*, 111(G4), G04004. <https://doi.org/10.1029/2005JG000134>
- Chasar, L. S., Chanton, J. P., Glaser, P. H., & Siegel, D. I. (2000). Methane concentration and stable isotope distribution as evidence of rhizospheric processes: Comparison of a fen and bog in the Glacial Lake Agassiz Peatland complex. *Annals of Botany*, 86(3), 655–663. <https://doi.org/10.1006/anbo.2000.1172>
- Chasmer, L., & Hopkinson, C. (2017). Threshold loss of discontinuous permafrost and landscape evolution. *Global Change Biology*, 23(7), 2672–2686. <https://doi.org/10.1111/gcb.13537>
- Chen, S., Arrouays, D., Mulder, V. L., Poggio, L., Minasny, B., Roudier, P., et al. (2022). Digital mapping of GlobalSoilMap soil properties at a broad scale: A review. *Geoderma*, 409, 115567. <https://doi.org/10.1016/j.geoderma.2021.115567>
- Coleman, D. D., Risatti, J. B., & Schoell, M. (1981). Fractionation of carbon and hydrogen isotopes by methane-oxidizing bacteria. *Geochimica et Cosmochimica Acta*, 45(7), 1033–1037. [https://doi.org/10.1016/0016-7037\(81\)90129-0](https://doi.org/10.1016/0016-7037(81)90129-0)
- Conrad, R. (2020). Methane production in soil environments—Anaerobic biogeochemistry and microbial life between flooding and desiccation. *Microorganisms*, 8(6), 881. <https://doi.org/10.3390/microorganisms8060881>
- Corbett, J. E., Tfaily, M. M., Burdige, D. J., Cooper, W. T., Glaser, P. H., & Chanton, J. P. (2013). Partitioning pathways of CO<sub>2</sub> production in peatlands with stable carbon isotopes. *Biogeochemistry*, 114(1–3), 327–340. <https://doi.org/10.1007/s10533-012-9813-1>
- Corbett, J. E., Tfaily, M. M., Burdige, D. J., Glaser, P. H., & Chanton, J. P. (2015). The relative importance of methanogenesis in the decomposition of organic matter in northern peatlands. *Journal of Geophysical Research: Biogeosciences*, 120(2), 280–293. <https://doi.org/10.1002/2014jg002797>
- Dalcin Martins, P., Hoyt, D. W., Bansal, S., Mills, C. T., Tfaily, M., Tangen, B. A., et al. (2017). Abundant carbon substrates drive extremely high sulfate reduction rates and methane fluxes in Prairie Pothole Wetlands. *Global Change Biology*, 23(8), 3107–3120. <https://doi.org/10.1111/gcb.13633>
- Deng, J., McCalley, C. K., Frohling, S., Chanton, J., Crill, P., Varner, R., et al. (2017). Adding stable carbon isotopes improves model representation of the role of microbial communities in peatland methane cycling. *Journal of Advances*, 9(2), 1412–1430. <https://doi.org/10.1002/2016MS000817>
- Douglas, P. M., Stratigopoulos, E., Park, S., & Phan, D. (2021). Geographic variability in freshwater methane hydrogen isotope ratios and its implications for global isotopic source signatures. *Biogeosciences*, 18(11), 3505–3527. <https://doi.org/10.5194/bg-18-3505-2021>
- Euskirchen, E. S., Edgar, C. W., Kane, E. S., Waldrop, M. P., Neumann, R. B., Manies, K. L., et al. (2024). Persistent net release of carbon dioxide and methane from an Alaskan lowland boreal peatland complex. *Global Change Biology*, 30(1), e17139. <https://doi.org/10.1111/gcb.17139>
- Fick, S. E., & Hijmans, R. J. (2017). WorldClim 2: New 1-km spatial resolution climate surfaces for global land areas. *International Journal of Climatology*, 37(12), 4302–4315. <https://doi.org/10.1002/joc.5086>
- Fisher, R. E., France, J. L., Lowry, D., Lanoisellé, M., Brownlow, R., Pyle, J. A., et al. (2017). Measurement of the <sup>13</sup>C isotopic signature of methane emissions from northern European wetlands. *Global Biogeochemical Cycles*, 31(3), 605–623. <https://doi.org/10.1002/2016gb005504>
- Frohling, S., Roulet, N., & Fuglestedt, J. (2006). How northern peatlands influence the Earth's radiative budget: Sustained methane emission versus sustained carbon sequestration. *Journal of Geophysical Research*, 111(G1), G01008. <https://doi.org/10.1029/2005JG000091>
- Galand, P. E., Yrjälä, K., & Conrad, R. (2010). Stable carbon isotope fractionation during methanogenesis in three boreal peatland ecosystems. *Biogeosciences*, 7(11), 3893–3900. <https://doi.org/10.5194/bg-7-3893-2010>
- Ganesan, A. L., Stell, A. C., Gedney, N., Comyn-Platt, E., Hayman, G., Rigby, M., et al. (2018). Spatially resolved isotopic source signatures of wetland methane emissions. *Geophysical Research Letters*, 45(8), 3737–3745. <https://doi.org/10.1002/2018GL077536>
- Heffernan, L., Cavaco, M. A., Bhatia, M. P., Estop-Aragonés, C., Knorr, K.-H., & Olefeldt, D. (2022). High peatland methane emissions following permafrost thaw: Enhanced acetoclastic methanogenesis during early successional stages. *Biogeosciences*, 19(12), 3051–3071. <https://doi.org/10.5194/bg-19-3051-2022>
- Heffernan, L., Estop-Aragonés, C., Knorr, K.-H., Talbot, J., & Olefeldt, D. (2020). Long-term impacts of permafrost thaw on carbon storage in peatlands: Deep losses offset by surficial accumulation. *Journal of Geophysical Research: Biogeosciences*, 125(3), e2019JG005501. <https://doi.org/10.1029/2019jg005501>
- Heiskanen, L., Tuovinen, J.-P., Räsänen, A., Virtanen, T., Juutinen, S., Lohila, A., et al. (2021). Carbon dioxide and methane exchange of a patterned subarctic fen during two contrasting growing seasons. *Biogeosciences*, 18(3), 873–896. <https://doi.org/10.5194/bg-18-873-2021>
- Hines, M. E., Duddleston, K. N., Rooney-Varga, J. N., Fields, D., & Chanton, J. P. (2008). Uncoupling of acetate degradation from methane formation in Alaskan wetlands: Connections to vegetation distribution. *Global Biogeochemical Cycles*, 22(2), GB2017. <https://doi.org/10.1029/2006GB002903>
- Hinzman, L. D., Viereck, L. A., Adams, P. C., Romanovsky, V. E., & Yoshikawa, K. (2006). *Climate and permafrost dynamics of the Alaskan boreal forest* (pp. 39–61). Alaska's Changing Boreal Forest. Retrieved from <https://books.google.com/books?hl=en&lr=&id=dHJCAAQBAJ&oi=fnd&pg=PA39&ots=WyUOVuLV0&sig=uZ6tOH8f1tqRKgRj9u42xaQIO1s>
- Hodgkins, S. B. (2016). *Changes in organic matter chemistry and methanogenesis due to permafrost thaw in a subarctic peatland*. ProQuest Dissertations Publishing. Print.
- Hodgkins, S. B., Chanton, J. P., Langford, L. C., McCalley, C. K., Saleska, S. R., Rich, V. I., et al. (2015). Soil incubations reproduce field methane dynamics in a subarctic wetland. *Biogeochemistry*, 126(1–2), 241–249. <https://doi.org/10.1007/s10533-015-0142-z>
- Hodgkins, S. B., Tfaily, M. M., McCalley, C. K., Logan, T. A., Crill, P. M., Saleska, S. R., et al. (2014). Changes in peat chemistry associated with permafrost thaw increase greenhouse gas production. *Proceedings of the National Academy of Sciences of the United States of America*, 111(16), 5819–5824. <https://doi.org/10.1073/pnas.1314641111>
- Horn, M. A., Matthies, C., Küsel, K., Schramm, A., & Drake, H. L. (2003). Hydrogenotrophic methanogenesis by moderately acid-tolerant methanogens of a methane-emitting acidic peat. *Applied and Environmental Microbiology*, 69(1), 74–83. <https://doi.org/10.1128/AEM.69.1.74-83.2003>
- Hornibrook, E. R. C. (2009). The stable carbon isotope composition of methane produced and emitted from northern peatlands. *Carbon Cycling in Northern Peatlands*, 184, 187–203. <https://doi.org/10.1029/2008GM000828>
- Hornibrook, E. R. C., Longstaffe, F. J., & Fyfe, W. S. (1997). Spatial distribution of microbial methane production pathways in temperate zone wetland soils: Stable carbon and hydrogen isotope evidence. *Geochimica et Cosmochimica Acta*, 61(4), 745–753. [https://doi.org/10.1016/S0016-7037\(96\)00368-7](https://doi.org/10.1016/S0016-7037(96)00368-7)

- Houweling, S., Dentener, F., & Lelieveld, J. (2000). Simulation of preindustrial atmospheric methane to constrain the global source strength of natural wetlands. *Journal of Geophysical Research*, *105*(D13), 17243–17255. <https://doi.org/10.1029/2000jd900193>
- Hugelius, G., Loisel, J., Chadburn, S., Jackson, R. B., Jones, M., MacDonald, G., et al. (2020). Large stocks of peatland carbon and nitrogen are vulnerable to permafrost thaw. *Proceedings of the National Academy of Sciences*, *117*(34), 20438–20446. <https://doi.org/10.1073/pnas.1916387117>
- Kane, E. S., Turetsky, M. R., Harden, J. W., McGuire, A. D., & Waddington, J. M. (2010). Seasonal ice and hydrologic controls on dissolved organic carbon and nitrogen concentrations in a boreal-rich fen. *Journal of Geophysical Research*, *115*(G4), G04012. <https://doi.org/10.1029/2010JG001366>
- Keller, J. K., & Bridgman, S. D. (2007). Pathways of anaerobic carbon cycling across an ombrotrophic-minerotrophic peatland gradient. *Limnology and Oceanography*, *52*(1), 96–107. <https://doi.org/10.4319/lo.2007.52.1.0096>
- Kelly, C. A., Dise, N. B., & Martens, C. S. (1992). Temporal variations in the stable carbon isotopic composition of methane emitted from Minnesota peatlands. *Global Biogeochemical Cycles*, *6*(3), 263–269. <https://doi.org/10.1029/92GB01478>
- Kuhn, M., Lundin, E. J., Giesler, R., Johansson, M., & Karlsson, J. (2018). Emissions from thaw ponds largely offset the carbon sink of northern permafrost wetlands. *Scientific Reports*, *8*(1), 9535. <https://doi.org/10.1038/s41598-018-27770-x>
- Kuhn, M. K. A., Varner, R. K., Bastviken, D., Crill, P., Intyre, S. M., Anthony, K. W., et al. (2021). BAWLD-CH: A comprehensive dataset of methane fluxes from boreal and Arctic ecosystems. *Earth System Science Data*, *13*(11), 5151–5189. <https://doi.org/10.5194/essd-2021-141Earth>
- Lansdown, J. M., Quay, P. D., & King, S. L. (1992). CH<sub>4</sub> production via CO<sub>2</sub> reduction in a temperate bog: A source of <sup>13</sup>C-depleted CH<sub>4</sub>. *Geochimica et Cosmochimica Acta*, *56*(9), 3493–3503. [https://doi.org/10.1016/0016-7037\(92\)90393-W](https://doi.org/10.1016/0016-7037(92)90393-W)
- Lawrence, D. M., Koven, C. D., Swenson, S. C., Riley, W. J., & Slater, A. G. (2015). Permafrost thaw and resulting soil moisture changes regulate projected high-latitude CO<sub>2</sub> and CH<sub>4</sub> emissions. *Environmental Research Letters: ERL [Web Site]*, *10*(9), 094011. <https://doi.org/10.1088/1748-9326/10/9/094011>
- Marushchak, M. E., Friborg, T., Biasi, C., Herbst, M., Johansson, T., Kiepe, I., et al. (2016). Methane dynamics in the subarctic tundra: Combining stable isotope analyses, plot- and ecosystem-scale flux measurements. *Biogeosciences*, *13*(2), 597–608. <https://doi.org/10.5194/bg-13-597-2016>
- Mazerolle, M. J., & Mazerolle, M. M. J. (2017). Package ‘AICcmodavg’. *R Package*, *281*, 1–220.
- McCalley, C. K., Woodcroft, B. J., Hodgkins, S. B., Wehr, R. A., Kim, E.-H., Mondav, R., et al. (2014). Methane dynamics regulated by microbial community response to permafrost thaw. *Nature*, *514*(7523), 478–481. <https://doi.org/10.1038/nature13798>
- Mikaloff Fletcher, S. E., Tans, P. P., Bruhwiler, L. M., Miller, J. B., & Heimann, M. (2004). CH<sub>4</sub> sources estimated from atmospheric observations of CH<sub>4</sub> and its <sup>13</sup>C/<sup>12</sup>C isotopic ratios: 1. Inverse modeling of source processes. *Global Biogeochemical Cycles*, *18*(4), GB4004. <https://doi.org/10.1029/2004gb002223>
- Miller, S. M., Worthy, D. E. J., Michalak, A. M., Wofsy, S. C., Kort, E. A., Havice, T. C., et al. (2014). Observational constraints on the distribution, seasonality, and environmental predictors of North American boreal methane emissions. *Global Biogeochemical Cycles*, *28*(2), 146–160. <https://doi.org/10.1002/2013gb004580>
- Monteil, G., Houweling, S., Dlugockenky, E. J., Maenhout, G., Vaughn, B. H., White, J. W. C., & Rockmann, T. (2011). Interpreting methane variations in the past two decades using measurements of CH<sub>4</sub> mixing ratio and isotopic composition. *Atmospheric Chemistry and Physics*, *11*(17), 9141–9153. <https://doi.org/10.5194/acp-11-9141-2011>
- Oh, Y., Bruhwiler, L., Lan, X., Basu, S., Shchuldt, K., Thoning, K., et al. (2023). *CarbonTracker CH<sub>4</sub> 2023*. NOAA Global Monitoring Laboratory. <https://doi.org/10.25925/40JT-QD67>
- Oh, Y., Zhuang, Q., Welp, L. R., Liu, L., Lan, X., Basu, S., et al. (2022). Improved global wetland carbon isotopic signatures support post-2006 microbial methane emission increase. *Communications Earth & Environment*, *3*(1), 1–12. <https://doi.org/10.1038/s43247-022-00488-5>
- Olefeldt, D., Hovemyr, M., Kuhn, M. K. A., Bastviken, D., Bohn, T. J., Connolly, J., et al. (2021a). The Boreal-Arctic Wetland and Lake Dataset (BAWLD). *Earth System Science Data*, *13*(11), 5127–5149. <https://doi.org/10.5194/essd-13-5127-2021>
- Olefeldt, D., Hovemyr, M., Kuhn, M. K. A., Bastviken, D., Bohn, T. J., Connolly, J., et al. (2021b). The fractional land cover estimates from the Boreal-Arctic Wetland and Lake Dataset (BAWLD) [Dataset]. *Arctic Data Center*. <https://doi.org/10.18739/A2C824F9X>
- Peltola, O., Vesala, T., Gao, Y., Rätty, O., Alekseychik, P., Aurela, M., et al. (2019). Monthly gridded data product of northern wetland methane emissions based on upscaling eddy covariance observations. *Earth System Science Data*, *11*(3), 1263–1289. <https://doi.org/10.5281/zenodo.2560163>
- Penger, J., Conrad, R., & Blaser, M. (2012). Stable carbon isotope fractionation by methylotrophic methanogenic archaea. *Applied and Environmental Microbiology*, *78*(21), 7596–7602. <https://doi.org/10.1128/aem.01773-12>
- Perryman, C. R., McCalley, C. K., Ernakovich, J. G., Lamit, L. J., Shorter, J. H., Lilleskov, E., & Varner, R. K. (2022). Microtopography matters: Belowground CH<sub>4</sub> cycling regulated by differing microbial processes in peatland hummocks and lawns. *Journal of Geophysical Research: Biogeosciences*, *127*(8), e2022JG006948. <https://doi.org/10.1029/2022jg006948>
- Perryman, C. R., McCalley, C. K., Malhotra, A., Fahnestock, M. F., Kashi, N. N., Bryce, J. G., et al. (2020). Thaw transitions and redox conditions drive methane oxidation in a permafrost peatland. *Journal of Geophysical Research: Biogeosciences*, *125*(3), e2019JG005526. <https://doi.org/10.1029/2019jg005526>
- Perryman, C. R., McCalley, C. K., Shorter, J. H., Perry, A. L., White, N., Dziurzynski, A., & Varner, R. K. (2023). Effect of drought and heavy precipitation on CH<sub>4</sub> emissions and δ<sup>13</sup>C-CH<sub>4</sub> in a northern temperate peatland. *Ecosystems*, *27*, 1–18. <https://doi.org/10.1007/s10021-023-00868-8>
- Piilo, S. R., Korhola, A., Heiskanen, L., Tuovinen, J.-P., Aurela, M., Jutinen, S., et al. (2020). Spatially varying peatland initiation, Holocene development, carbon accumulation patterns and radiative forcing within a subarctic fen. *Quaternary Science Reviews*, *248*, 106596. <https://doi.org/10.1016/j.quascirev.2020.106596>
- Pirinen, P. (2012). *Climatological Statistics of Finland 1981–2010*. Finnish Meteorological Institute.
- Popp, T. J., Chanton, J. P., Whiting, G. J., & Grant, N. (1999). Methane stable isotope distribution at a Carex dominated fen in north central Alberta. *Global Biogeochemical Cycles*, *13*(4), 1063–1077. <https://doi.org/10.1029/1999gb900060>
- Popp, T. J., Chanton, J. P., Whiting, G. J., & Grant, N. (2000). Evaluation of methane oxidation in the rhizosphere of a Carex dominated fen in northcentral Alberta, Canada. *Biogeochemistry*, *51*(3), 259–281. <https://doi.org/10.1023/A:1006452609284>
- R Core Team. (2023). *R: A language and environment for statistical computing*. R Foundation for Statistical Computing. Retrieved from <https://www.R-project.org/>
- Rigby, M., Manning, A. J., & Prinn, R. G. (2012). The value of high-frequency, high-precision methane isotopologue measurements for source and sink estimation. *Journal of Geophysical Research*, *117*(D12), D12312. <https://doi.org/10.1029/2011jd017384>



- Robison, A. L., Wollheim, W. M., Perryman, C. R., Cotter, A. R., Mackay, J. E., Varner, R. K., et al. (2022). Dominance of diffusive methane emissions from lowland headwater streams promotes oxidation and isotopic enrichment. *Frontiers of Environmental Science & Engineering in China*, 9, 791305. <https://doi.org/10.3389/fenvs.2021.791305>
- Rupp, D., Kane, E. S., Dieleman, C., Keller, J. K., & Turetsky, M. (2019). Plant functional group effects on peat carbon cycling in a boreal rich fen. *Biogeochemistry*, 144(3), 305–327. <https://doi.org/10.1007/s10533-019-00590-5>
- Rydin, H., Jeglum, J. K., & Bennett, K. D. (2013). *The biology of peatlands* (2nd ed.). OUP Oxford.
- Schulze, C., Sonnentag, O., Voigt, C., Thompson, L., van Delden, L., Heffernan, L., et al. (2023). Nitrous oxide fluxes in permafrost peatlands remain negligible after wildfire and thermokarst disturbance. *Journal of Geophysical Research: Biogeosciences*, 128(4), e2022JG007322. <https://doi.org/10.1029/2022jg007322>
- Stevens, C. M., & Engelkemeir, A. (1988). Stable carbon isotopic composition of methane from some natural and anthropogenic sources. *Journal of Geophysical Research*, 93(D1), 725–733. <https://doi.org/10.1029/JD093iD01p00725>
- Tahvanainen, T., & Haraguchi, A. (2013). Effect of pH on phenol oxidase activity on decaying Sphagnum mosses. *European Journal of Soil Biology*, 54, 41–47. <https://doi.org/10.1016/j.ejsobi.2012.10.005>
- Throckmorton, H. M., Heikoop, J. M., Newman, B. D., Altmann, G. L., Conrad, M. S., Muss, J. D., et al. (2015). Pathways and transformations of dissolved methane and dissolved inorganic carbon in Arctic tundra watersheds: Evidence from analysis of stable isotopes. *Global Biogeochemical Cycles*, 29(11), 1893–1910. <https://doi.org/10.1002/2014gb005044>
- Treat, C. C., Bloom, A. A., & Marushchak, M. E. (2018). Nongrowing season methane emissions—A significant component of annual emissions across northern ecosystems. *Global Change Biology*, 24(8), 3331–3343. <https://doi.org/10.1111/gcb.14137>
- Treat, C. C., Bubier, J. L., Varner, R. K., & Crill, P. M. (2007). Timescale dependence of environmental and plant-mediated controls on CH<sub>4</sub> flux in a temperate fen. *Journal of Geophysical Research*, 112(G1), G01014. <https://doi.org/10.1029/2006jg000210>
- Turetsky, M. R., Abbott, B. W., Jones, M. C., Anthony, K. W., Olefeldt, D., Schuur, E. A. G., et al. (2020). Carbon release through abrupt permafrost thaw. *Nature Geoscience*, 13(2), 138–143. <https://doi.org/10.1038/s41561-019-0526-0>
- Turetsky, M. R., Treat, C. C., Waldrop, M. P., Waddington, J. M., Harden, J. W., & McGuire, A. D. (2008). Short-term response of methane fluxes and methanogen activity to water table and soil warming manipulations in an Alaskan peatland. *Journal of Geophysical Research*, 113(G3), G00A10. <https://doi.org/10.1029/2007jg000496>
- Varner, R. K., Crill, P. M., Froelking, S., McCalley, C. K., Burke, S. A., Chanton, J. P., et al. (2022). Permafrost thaw driven changes in hydrology and vegetation cover increase trace gas emissions and climate forcing in Stordalen Mire from 1970 to 2014. *Philosophical Transactions of the Royal Society A*, 380(2215), 20210022. <https://doi.org/10.1098/rsta.2021.0022>
- Waldron, S., Hall, A. J., & Fallick, A. E. (1999). Enigmatic stable isotope dynamics of deep peat methane. *Global Biogeochemical Cycles*, 13(1), 93–100. <https://doi.org/10.1029/1998GB900002>
- Waldron, S., Lansdown, J. M., Scott, E. M., Fallick, A. E., & Hall, A. J. (1999). The global influence of the hydrogen isotope composition of water on that of bacteriogenic methane from shallow freshwater environments. *Geochimica et Cosmochimica Acta*, 63(15), 2237–2245. [https://doi.org/10.1016/S0016-7037\(99\)00192-1](https://doi.org/10.1016/S0016-7037(99)00192-1)
- Whiticar, M. J. (1999). Carbon and hydrogen isotope systematics of bacterial formation and oxidation of methane. *Chemical Geology*, 161(1–3), 291–314. [https://doi.org/10.1016/S0009-2541\(99\)00092-3](https://doi.org/10.1016/S0009-2541(99)00092-3)
- Whiticar, M. J., Faber, E., & Schoell, M. (1986). Biogenic methane formation in marine and freshwater environments: CO<sub>2</sub> reduction vs. acetate fermentation—Isotope evidence. *Geochimica et Cosmochimica Acta*, 50(5), 693–709. [https://doi.org/10.1016/0016-7037\(86\)90346-7](https://doi.org/10.1016/0016-7037(86)90346-7)
- Wik, M., Thornton, B. F., Varner, R. K., McCalley, C., & Crill, P. M. (2020). Stable methane isotopologues from northern lakes suggest that ebullition is dominated by sub-lake scale processes. *Journal of Geophysical Research: Biogeosciences*, 125(10), e2019JG005601. <https://doi.org/10.1029/2019jg005601>
- Zhang, H., Väiliranta, M., Piilo, S., Amesbury, M. J., Aquino-López, M. A., Roland, T. P., et al. (2020). Decreased carbon accumulation feedback driven by climate-induced drying of two southern boreal bogs over recent centuries. *Global Change Biology*, 26(4), 2435–2448. <https://doi.org/10.1111/gcb.15005>
- Zhang, H., Väiliranta, M., Swindles, G. T., Aquino-López, M. A., Mullan, D., Tan, N., et al. (2022). Recent climate change has driven divergent hydrological shifts in high-latitude peatlands. *Nature Communications*, 13(1), 4959. <https://doi.org/10.1038/s41467-022-32711-4>